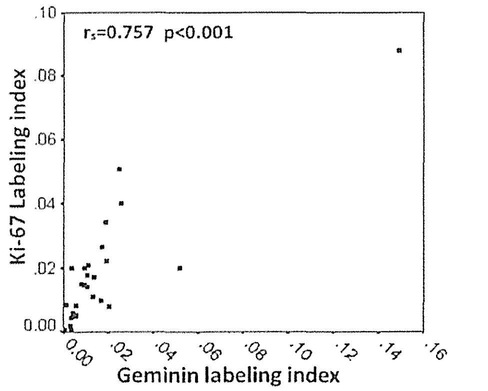

Geminin LI	Median; 1.0 % (Range; 0.05-14.9)	< 2% / ≥ 2%	22 (81.5%) / 5 (18.5%)
Ki-67 LI	Median; 1.5 % (Range; 0.02-8.8)	< 2% / ≥ 2%	19 (70.4%) / 8 (29.6%)

FIGURE 2. Scatterplot of the geminin LI and the Ki-67 LI (top) shows a positive correlation between the 2 LIs (Spearman rank correlation coefficient; $r_s = 0.757$; $P < 0.001$). The geminin expression level was lower than the Ki-67 expression level (bottom).

CI, 1.163–302.6; $P = 0.039$), a metastasis (HR, 10.469; 95% CI, 1.103–102.77; $P = 0.041$), a Ki-67 LI greater than 2.0% (HR, 6.182; 95% CI, 1.221–31.298; $P = 0.028$), a geminin LI greater than 2.0% (HR, 13.709; 95% CI, 1.919–97.739; $P = 0.009$), an AJCC stage of IIA or greater (HR, 8.758; 95% CI, 1.483–51.716; $P = 0.017$), and an ENETS stage of IIb or greater (HR, 16.793; 95% CI, 1.834–153.738; $P = 0.013$) were significantly correlated with recurrence. A multivariate Cox regression analysis revealed that none of these factors were independent prognostic factors. The Kaplan-Meier curves consistently exhibited a more significant relationship with the disease-free survival period after surgery for geminin (log rank, $P < 0.001$) than for Ki-67 (log rank, $P = 0.012$) (Fig. 4).

Concordance of Positivity Between Geminin and Ki-67 Stains

The immunoreactions were quantified using the CIE LAB color system. The color difference quotation was used to evaluate the positivity of the 2 stains. The color difference, ΔE, and a geminin-stained image are shown in Figure 5. The ΔE values

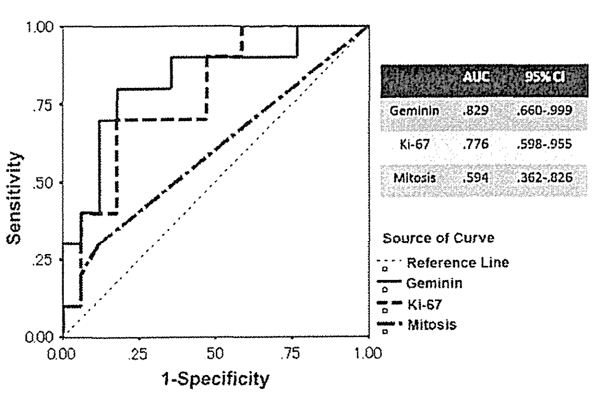

FIGURE 3. Receiver operating characteristic curves comparing the predictive value of the geminin LI to that of the Ki-67 LI or the mitosis count for determining the presence of metastasis.

TABLE 2. Univariate Cox Regression Analysis of Risk of Recurrence After Surgery

Variables	HR	95% CI	*P*
Diameter ≥2 cm	1.209	0.221–6.627	0.827
Mitosis ≥2 per 10 HPFs	10.204	1.684–61.834	0.012
v(+) or ly(+)	0.813	0.114–5.807	0.813
pn(+)	3.615	0.375–34.837	0.266
s(+) or rp(+)	2.068	0.411–10.4	0.378
Local invasion (+)	18.762	1.163–302.6	0.039
Metastasis (+)	10.469	1.103–102.77	0.041
Ki-67 LI >2.0%	6.182	1.221–31.298	0.028
Geminin LI >2.0%	13.709	1.919–97.739	0.009
WHO grade G2	2772.5	$0.000–95.889 \times 10^7$	0.429
AJCC stage ≥IIA	8.758	1.483–51.716	0.017
ENETS stage ≥IIb	16.793	1.834–153.74	0.013

Local invasion indicates (+), presence of local invasion; ly(+), presence of lymphatic invasion; metastasis (+), presence of metastasis; pn(+), presence of peri-neural invasion; rp(+), presence of retroperitoneal invasion; s(+), presence of serosal invasion; v(+), presence of venous invasion.

corresponded with the optical intensity of the positive cells. The same consistency was observed for the images with Ki-67 staining (data was not shown). The distributions of ΔE in the geminin and Ki-67 staining images are shown in Figure 6. $\Delta E = 0$ signified no color difference from negative cells, and the left side of the histogram's distribution indicates the number of cells with equivocal positivity. A larger ΔE reflects a greater color disparity between the positive and negative cells. The medians (ranges) of the ΔE values for geminin and Ki-67 staining were

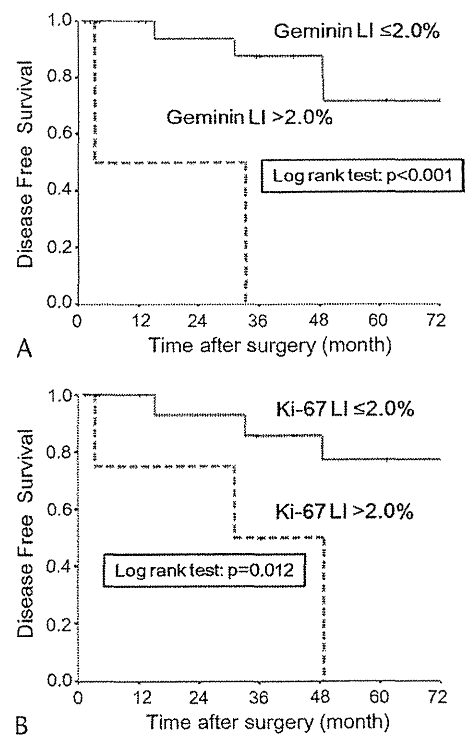

FIGURE 4. Disease-free survival period after surgery according to the geminin LI (A) and the Ki-67 LI (B).

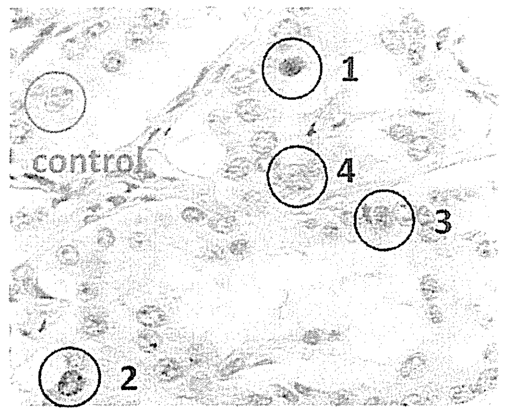

#	L* value	a* value	b* value	ΔE
1	65.17	-1.22	15.30	26.22
2	67.90	7.30	11.63	21.87
3	77.14	5.71	5.74	11.10
4	82.30	3.29	-0.71	2.51
Ctr	83.94	2.82	-2.55	-

FIGURE 5. The color difference ΔE in geminin stain is shown. ΔE values were calculated from the difference of L*a*b* values between positive cells (in numbered red circles) and a negative cell (in green circle).

16.12 (5.8–41.8) and 13.17 (3.4–37.9), respectively. The ΔE for the geminin stain was significantly larger than that for the Ki-67 stain ($P < 0.001$).

DISCUSSION

The criteria used to predict the outcome of patients with PNET has been simplified in the 2010 WHO classification.[6] Pancreatic neuroendocrine tumors are divided into well-differentiated NETs and poorly differentiated neuroendocrine carcinoma (NEC). The definition of NEC is the presence of more than 20 mitoses per 10 HPFs. Neuroendocrine tumors were further subcategorized as low-grade NET (G1), characterized by the presence of 0 to 1 mitoses and a Ki-67 LI of 0% to 2%, and intermediate-grade NET (G2), characterized as 2 to 20 mitoses per 10 HPFs and a Ki-67 LI of 3% to 20%. Actually, immunohistochemical staining for Ki-67 has been the most reliable modality for assessing the proliferative activity.[2,3,7] In addition, staging has been noted to be an independent prognostic indicator, and the AJCC staging manual and the staging classification proposed by the ENETS are thought to be useful for predicting the prognosis of patients with PNET. In the present study, 19 and 8 cases were classified as G1 and G2, respectively. No cases of NEC were seen, consistent with the presence of only 1 tumor-related death. Regarding recurrence after radical resection, this grading system is not a reliable prognostic factor (Table 2). Unlike the WHO grading, however, both the AJCC and ENETS stagings are significantly correlated with recurrence; similarly, the superiority of these stagings to anticipate disease-free survival has been previously reported.[25] The present analysis suggested that local spread beyond the pancreas might be a key event.

The usefulness of geminin staining to predict the outcome of several neoplasms has been demonstrated using retrospective analyses.[17–22] The present study also indicated that geminin expression was a more useful indicator of disease-free survival than not only Ki-67 expression but also AJCC and ENETS staging (Table 2). Geminin expression is specifically limited during the S, G2, and early M phases, and it probably reflects the proliferative activity more precisely than these other factors. Indeed, the number of positive tumor cells for geminin was significantly smaller than that for Ki-67. Although the survival analysis using Kaplan-Meier curves suggested that the geminin LI was more associated with the prognosis than the Ki-67 LI (Fig. 4), the present study has a limitation to evaluate the prognosis in accordance with the small number of cases. Further analyses of a larger population is needed to determine the prognostic use of the geminin LI. Moreover, the mechanism by which geminin expression contributes to the aggressiveness of neoplasms remains unknown. The inhibition of Cdt1 by geminin has been regarded as a pivotal event in the licensing of DNA replication, so an increase in Cdt1 inhibition biologically results in cell cycle arrest. This discrepancy between geminin expression and cell proliferation remains to be explained. The predictive superiority of the geminin LI to the Ki-67 LI in the present analysis may depend on some aspect of the malignant potential other than the proliferative activity.

In addition, the immunoreactivity of geminin staining in each tumor cell was relatively clear, whereas weak positivity for Ki-67 staining was observed in some tumor cells (Fig. 1). Thus, fewer intraobserver and interobserver differences between pathologists or institutions can be expected using the geminin LI. Actually, the difficulty in grading PNETs has been attributed to the need for concordance, along with the lower frequencies of proliferative marker positivity in PNETs. In the present study, we performed a color difference quotation analysis using the CIE LAB color system. Several color analyses have reported that the

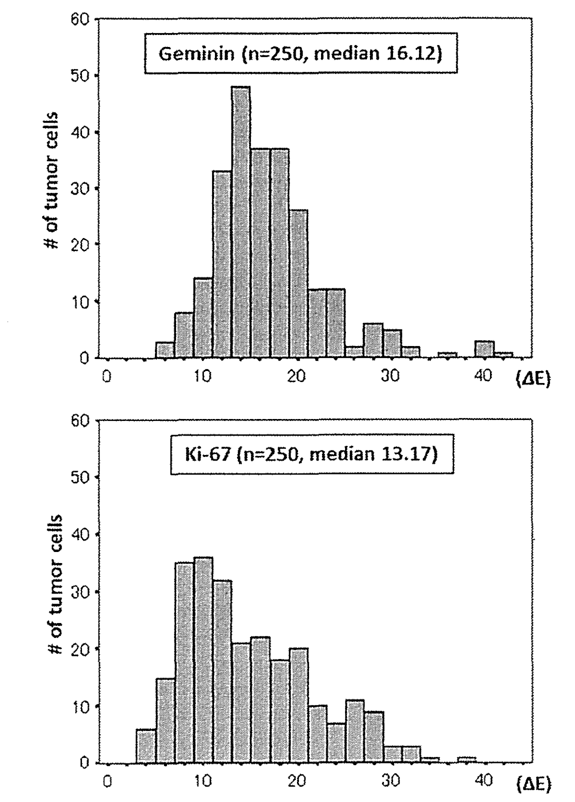

FIGURE 6. The distribution of each ΔE in geminin and Ki-67 stain is shown. The difference of each ΔE was evaluated as statistically significant ($P < 0.001$) using the Mann-Whitney U test.

color parameters of the CIE LAB color system are closely related to the psychophysical characteristics of color perception.[26–28] This analysis was the first application of the CIE LAB color system for the quantification of immunohistochemical positivity. As shown in Figure 5, a precise correspondence between ΔE and the optical color intensities was observed. Furthermore, the ΔE for geminin staining was larger than that for Ki-67 staining. These results suggest that a greater concordance was achieved using the geminin LI rather than the Ki-67 LI. The use of the color difference quotation enabled subjective optical intensities to be measured as absolute values, and no inconsistencies with regard to determining positivity were encountered. Thus, the CIE LAB color system may be a promising tool for making objective histopathologic assessments.

Pancreatic neuroendocrine tumor constitutes a heterogeneous group of rare neoplasms. Recent advances in abdominal imaging techniques have increased the detection of incidental nonfunctional PNET. In particular, endoscopic ultrasound and endoscopic ultrasound–guided fine needle aspiration biopsy procedures have drastically improved diagnostic accuracy.[29] Nowadays, minimally invasive surgery is usually recommended as a pancreas-preserving maneuver.[30] Therefore, accurate estimates of the malignant potential before surgery are becoming increasingly important for optimal patient management. Despite the importance of such estimations, pretreatment evaluations remain difficult. Only microscopic observations are acceptable for tumor grading and staging because PNET can exhibit heterogeneous biological behavior even within the same tumor. In the present study, a heterogeneous expression level was observed throughout the tumor for both geminin and Ki-67 staining. The use of geminin expression for the assessment of biopsy samples or aspirated specimens was not evaluated in the present study. Thus, the establishment of a preoperative classification based on geminin expression will require further research.

In conclusion, the geminin expression level in PNETs was correlated with the disease-free survival period after curative resection. The geminin LI may be more useful than the Ki-67 LI for predicting postoperative outcome.

ACKNOWLEDGMENT

The authors thank Dr Hiroshi Yamaguchi and Dr Toshio Ohmori, Imaging Technology Center, FUJIFILM Corp, Minamiashigara, Japan, for their technical advice.

REFERENCES

1. Imamura M. Recent standardization of treatment strategy for pancreatic neuroendocrine tumors. *World J Gastroenterol.* 2010;16(36):4519–4525.
2. Ferrone CR, Tang LH, Tomlinson J, et al. Determining prognosis in patients with pancreatic endocrine neoplasms: can the WHO classification system be simplified? *J Clin Oncol.* 2007;25(35): 5609–5615.
3. Pelosi G, Bresaola E, Bogina G, et al. Endocrine tumors of the pancreas: Ki-67 immunoreactivity on paraffin sections is an independent predictor for malignancy: a comparative study with proliferating-cell nuclear antigen and progesterone receptor protein immunostaining, mitotic index, and other clinicopathologic variables. *Hum Pathol.* 1996;27(11):1124–1134.
4. Hochwald SN, Zee S, Conlon KC, et al. Prognostic factors in pancreatic endocrine neoplasms: an analysis of 136 cases with a proposal for low-grade and intermediate-grade groups. *J Clin Oncol.* 2002;20(11):2633–2642.
5. Phan GQ, Yeo CJ, Hruban RH, et al. Surgical experience with pancreatic and peripancreatic neuroendocrine tumors: review of 125 patients. *J Gastrointest Surg.* 1998;2(5):473–482.
6. Bosman FT, Carneiro F, Hruban RH, eds. *WHO Classification of Tumours of the Digestive System.* 4th ed. Lyon, France: IARC; 2010.
7. Ekeblad S, Skogseid B, Dunder K, et al. Prognostic factors and survival in 324 patients with pancreatic endocrine tumor treated at a single institution. *Clin Cancer Res.* 2008;14(23):7798–7803.
8. La Rosa S, Sessa F, Capella C, et al. Prognostic criteria in nonfunctioning pancreatic endocrine tumours. *Virchows Arch.* 1996;429(6):323–333.
9. Gentil Perret A, Mosnier JF, Buono JP, et al. The relationship between MIB-1 proliferation index and outcome in pancreatic neuroendocrine tumors. *Am J Clin Pathol.* 1998;109(3):286–293.
10. Clarke MR, Baker EE, Weyant RJ, et al. Proliferative activity in pancreatic endocrine tumors: association with function, metastases, and survival. *Endocr Pathol.* 1997;8(3):181–187.
11. Gerdes J, Lemke H, Baisch H, et al. Cell cycle analysis of a cell proliferation–associated human nuclear antigen defined by the monoclonal antibody Ki-67. *J Immunol.* 1984;133(4):1710–1715.
12. Scholzen T, Gerdes J. The Ki-67 protein: from the known and the unknown. *J Cell Physiol.* 2000;182(3):311–322.
13. Wohlschlegel JA, Kutok JL, Weng AP, et al. Expression of geminin as a marker of cell proliferation in normal tissues and malignancies. *Am J Pathol.* 2002;161(1):267–273.
14. Takeda DY, Dutta A. DNA replication and progression through S phase. *Oncogene.* 2005;24(17):2827–2843.
15. McGarry TJ, Kirschner MW. Geminin, an inhibitor of DNA replication, is degraded during mitosis. *Cell.* 1998;93(6):1043–1053.
16. Wohlschlegel JA, Dwyer BT, Dhar SK, et al. Inhibition of eukaryotic DNA replication by geminin binding to Cdt1. *Science.* 2000;290(5500):2309–2312.
17. Gonzalez MA, Tachibana KE, Chin SF, et al. Geminin predicts adverse clinical outcome in breast cancer by reflecting cell-cycle progression. *J Pathol.* 2004;204(2):121–130.
18. Dudderidge TJ, Stoeber K, Loddo M, et al. Mcm2, geminin, and KI67 define proliferative state and are prognostic markers in renal cell carcinoma. *Clin Cancer Res.* 2005;11(7):2510–2517.
19. Dudderidge TJ, McCracken SR, Loddo M, et al. Mitogenic growth signalling, DNA replication licensing, and survival are linked in prostate cancer. *Br J Cancer.* 2007;96(9):1384–1393.
20. Yamazaki M, Fujii S, Murata Y, et al. High expression level of geminin predicts a poor clinical outcome in salivary gland carcinomas. *Histopathology.* 2010;56(7):883–892.
21. Haruki T, Shomori K, Hamamoto Y, et al. Geminin expression in small lung adenocarcinomas: implication of prognostic significance. *Lung Cancer.* 2011;71(3):356–362.
22. Shomori K, Nishihara K, Tamura T, et al. Geminin, Ki67, and minichromosome maintenance 2 in gastric hyperplastic polyps, adenomas, and intestinal-type carcinomas: pathobiological significance. *Gastric Cancer.* 2010;13(3):177–185.
23. Edge SB, Byrd DR, Compton CC, et al, eds. *AJCC Cancer Staging Manual.* 7th ed. New York, NY: Springer; 2010.
24. Rindi G, Kloppel G, Alhman H, et al. TNM staging of foregut (neuro)endocrine tumors: a consensus proposal including a grading system. *Virchows Arch.* 2006;449(4):395–401.
25. La Rosa S, Klersy C, Uccella S, et al. Improved histologic and clinicopathologic criteria for prognostic evaluation of pancreatic endocrine tumors. *Hum Pathol.* 2009;40(1):30–40.
26. Jorn D, Waddell JN, Swain MV. The influence of opaque application methods on the bond strength and final shade of PFM restorations. *J Dent.* 2010;38(suppl 2):e143–e149.
27. Kim JY, Kim JW, Seo SH, et al. A novel consistent photomicrography technique using a reference slide made of neutral density filter. *Microsc Res Tech.* 2011;74(5):397–400.
28. Kinnunen J, Jurvelin JS, Makitalo J, et al. Optical spectral imaging of degeneration of articular cartilage. *J Biomed Opt.* 2010;15(4):046024.
29. Figueiredo FA, Giovannini M, Monges G, et al. Pancreatic endocrine tumors: a large single-center experience. *Pancreas.* 2009;38(8): 936–940.
30. Casadei R, Ricci C, Rega D, et al. Pancreatic endocrine tumors less than 4 cm in diameter: resect or enucleate? A single-center experience. *Pancreas.* 2010;39(6):825–828.

Prognostic Impact of CD204-Positive Macrophages in Lung Squamous Cell Carcinoma

Possible Contribution of Cd204-Positive Macrophages to the Tumor-Promoting Microenvironment

Shunki Hirayama, MD,†‡ Genichiro Ishii, MD, PhD,* Kanji Nagai, MD, PhD,† Shotaro Ono, MD,*‡ Motohiro Kojima, MD, PhD,* Chisako Yamauchi MD, PhD,* Keiju Aokage, MD, PhD,† Tomoyuki Hishida, MD, PhD,† Junji Yoshida, MD, PhD,† Kenji Suzuki, MD, PhD,‡ and Atsushi Ochiai, MD, PhD**

Introduction: Tumor-associated macrophages (TAMs) are recruited into cancer-induced stroma and produce a specific microenvironment for cancer progression. CD204 (+) TAMs are reportedly related to tumor progression and clinical outcome in some tumors. The aim of this study was to clarify the correlation between CD204 (+) TAMs and the clinicopathological features of lung squamous cell carcinoma.

Methods: We investigated the relationships between the numbers of CD204 (+) TAMs and clinicopathological factors, microvessel density, and the numbers of Foxp3 (+) lymphocytes in 208 consecutively resected cases. We also examined the relationships between the numbers of CD204 (+) TAMs and the expression levels of cytokines involved in the migration and differentiation of CD204 (+) TAMs.

Results: A high number of CD204 (+) TAMs in the stroma was significantly correlated with an advanced p-stage, T factor, N factor, and the presence of vascular and pleural invasion. A high number of CD204 (+) TAMs in the stroma was also a significant prognostic factor for all p-stages and p-stage I. Moreover, the numbers of CD204 (+) TAMs were correlated with the microvessel density and the numbers of Foxp3 (+) lymphocytes. A high number of CD204 (+) TAMs was strongly correlated with the tissue expression level of monocyte chemoattractant protein-1. CD204 (+) TAMs were shown to be significant independent prognostic factors in a multivariate analysis.

Conclusions: CD204 (+) TAMs were an independent prognostic factor in lung squamous cell carcinoma. CD204 (+) TAMs, along with other tumor-promoting stromal cells such as regulatory T cells and endothelial cells, may create tumor-promoting microenvironments.

Departments of *Pathology and †Thoracic Oncology, Research Center for Innovative Oncology, National Cancer Center Hospital East, Kashiwa, Chiba, Japan; ‡Department of General Thoracic Surgery, Juntendo University School of Medicine, Tokyo, Japan.

Disclosure: The authors declare no conflict of interest.

Address for correspondence: Genichiro Ishii, MD, PhD, or Atsushi Ochiai, MD, PhD, Pathology Division, Research Center for Innovative Oncology, National Cancer Center Hospital East, Kashiwa, Chiba, 277-8577, Japan. E-mail: gishii@east.ncc.go.jp or aochiai @east.ncc.go.jp

ISSN: 1556-0864/12/0712-1790

Key Words: CD204, Tumor associated macrophages, Non–small-cell lung carcinoma, Squamous cell carcinoma.

(*J Thorac Oncol.* 2012;7: 1790–1797)

The tumor microenvironment is composed of not only tumor cells, but also stromal cells including macrophages, lymphocytes, fibroblasts, and endothelial cells. Stromal cells are known to interact with cancer cells and to produce a specific microenvironment capable of influencing tumor progression.[1] In the host immune system in cancer tissue, tumor-associated macrophages (TAMs) as well as cancer-associated fibroblasts are important components of the tumor microenvironment, and some kinds of macrophages are known to act on tumor progression.[2] Recent immunological studies have identified two different functions of polarized macrophage activation, as exhibited by classically activated (M1) and alternatively activated (M2) macrophage phenotypes.[3,4] These subpopulations of macrophages have different receptor expression patterns and different cytokine and chemokine productions. M1-polarized macrophages have an interleukin (IL)-12^{high}, IL-23^{high}, IL-10^{low} phenotype and defend the body against pathogens and tumor cells by inducing interferon-gamma and producing tumor necrosis factor α and nitric oxide. M1-polarized macrophages reportedly play a role in tumor suppression. However, M2-polarized macrophages have an IL-12^{low}, IL-23^{low}, IL-10^{high} phenotype and have high expression levels of class A scavenger receptor (CD204) and mannose receptor (CD163).[5–7] M2-polarized macrophages play a role in tumor-supportive functions, such as tumorigenesis, angiogenesis, matrix remodeling, and immune-suppression.[8] Recent studies have reported that the number of CD204-positive TAMs within a primary tumor is related to tumor progression and outcome in glioma, ovarian epithelial tumors, pancreatic cancer, and lung adenocarcinoma.[6,9–11]

Although squamous cell carcinoma of the lung is second only to adenocarcinoma of the lung, its treatmentt has not yet been sufficiently effective. Recently, the development of cancer therapy targeting cancer stromal cells has been proposed.[12] In the current study, we examined whether the numbers of CD204 (+) TAMs recruited into the cancer tissue are related to clinicopathological factors of lung squamous cell carcinoma. Furthermore, we examined the matching correlations between CD204 (+) TAMs and other types of cancer stromal cells, including regulatory T cells and endothelial cells.

MATERIALS AND METHODS

Patients

Between January 2000 and December 2006, a total of 255 patients with lung squamous cell carcinoma underwent surgery with curative intent at our hospital. We excluded 47 cases with poor-quality surgical specimens, and the remaining 208 cases were included in this study. The median follow-up period was 5.7 years.

Histopathology Studies

Surgical specimens were fixed in 10% formalin or methanol and embedded in paraffin. Sections that are 4-μm–thick were stained using the hematoxylin and eosin method. Vascular invasion and pleural invasion were evaluated using the Verhoeff-van-Gieson method. The histologic diagnoses were based on the third revised World Health Organization histologic classification. Disease stages were based on the 7th edition of TNM classification.

Evaluation of Clinicopathological Factors

The clinical characteristics were retrieved from the available clinical records. The following clinicopathological factors were investigated retrospectively to assess their impact on survival: age, sex, smoking history, pathologic stage, pathologic T status, pathologic nodal involvement, lymphatic permeation, vascular invasion, and pleural invasion.

Antibodies and Immunohistochemistry

The slides were deparaffinized with xylene, rehydrated, and antigen-retrieved in a microwave oven for 20 minutes. After the inhibition of endogenous peroxidase activity, individual slides were then incubated overnight at 4°C with mouse antihuman CD204 antibody (Scavenger Receptor class A-E5; Transgenic, Japan) at a final dilution of 1:400, mouse antihuman CD34 antibody (QBEND/10; Acris Antibodies, Herford, Germany) at a final dilution of 1:400, and mouse monoclonal antihuman Foxp3 antibody (236A/E7; Abcam, Japan) at a final dilution of 1:150. The slides were then incubated with EnVision (Dako, Denmark), and the color reaction was developed in 2% 3, 3-diaminobenzidine in 50mM Tris-buffer (pH7.6) containing 0.3% hydrogen peroxidase. Finally, the sections were counterstained with Meyer hematoxylin.

Evaluation of Immunohistochemistry

Two pathologists (S.H. and G.I.) selected a hot spot within a section and counted the CD204 (+) TAMs in the cancer stroma and nest in five high-power microscopic fields (×400; 0.0625 mm^2). The average counts were recorded and cases were divided into two groups with low and high numbers of CD204 (+) TAMs according to the median value. The absolute number of Foxp3-positive lymphocytes in the stroma, was counted in five randomly selected high-power microscopic fields (×400; 0.0625 mm^2), and the average counts were recorded. As for the microvessel density (MVD), the five most vascular areas (hot spots) in the invasive foci within a section were selected, and vessels labeled with anti-CD34 monoclonal antibody were counted in five high-power microscopic fields (×400; 0.0625 mm^2). The average counts were recorded as the MVD. In these studies, we selected areas in the central area within a cancer tissue, and necrotic areas were excluded.

Tissue Samples, RNA Extraction, Reverse Transcription, and Real-Time Polymerase Chain Reaction

Total RNA was extracted from 13 lung squamous cell carcinoma cases.. Samples of both cancer tissue and noncancerous tissue were collected and immediately homogenized in QIAzol Lysis reagent (QIAGEN, CA) with Tissue Lyser II (QIAGEN) and stored at −80°C until use. The total RNA was isolated from the tissues using a QIAshredderTM (250) (QIAGEN) and an RNeasy Mini Kit (250) (QIAGEN) according to the manufacturer's instructions. The RNA was reverse transcribed to synthesize cDNA using a primerscript RT reagent kit (Takara Biochemicals, Osaka, Japan). To quantitatively compare the mRNA levels of each cytokine, we performed a real-time polymerase chain reaction using SYBR Premix Ex TaqII (Takara) with the Smart Cycler II (Takara). The sense and antisense primers used for quantitative amplification of the cytokine mRNAs and for amplification of glyceraldehyde-3-phosphate dehydrogenase as an internal control are shown in (Supplemental Table 1, Supplemental Digital Content 1, http://links.lww.com/JTO/A347). The amount of template cDNA was expressed by the threshold cycles (G), determined from the amplification curve (exponential curve), and the threshold level for the detection of the polymerase chain reaction product. The expression level of each gene was reported as the ratio of its expression to the level of glyceraldehyde-3-phosphate dehydrogenase gene expression in the same sample. The ratio between the level of cytokine expression in the cancer tissue to the level of expression in the noncancerous tissue was calculated for each case. The median number of CD204 (+) TAMs was used to divide the cases into high and low CD204 (+) TAM groups.

Statistical Analysis

The distributions of CD204 (+) TAMs in the stroma and MVD and Foxp3-positive lymphocytes were tested for correlations by calculating the Spearman rank correlation coefficients. Overall survival (OS) was measured from the date of surgery until the date of death from any cause or to the date on which the patient was last known to be alive. Recurrence-free survival (RFS) was measured from the date of surgery until the date of recurrence or until the date the patient was last known to be disease free. Survival curves were estimated using the Kaplan–Meier method, and differences in survival

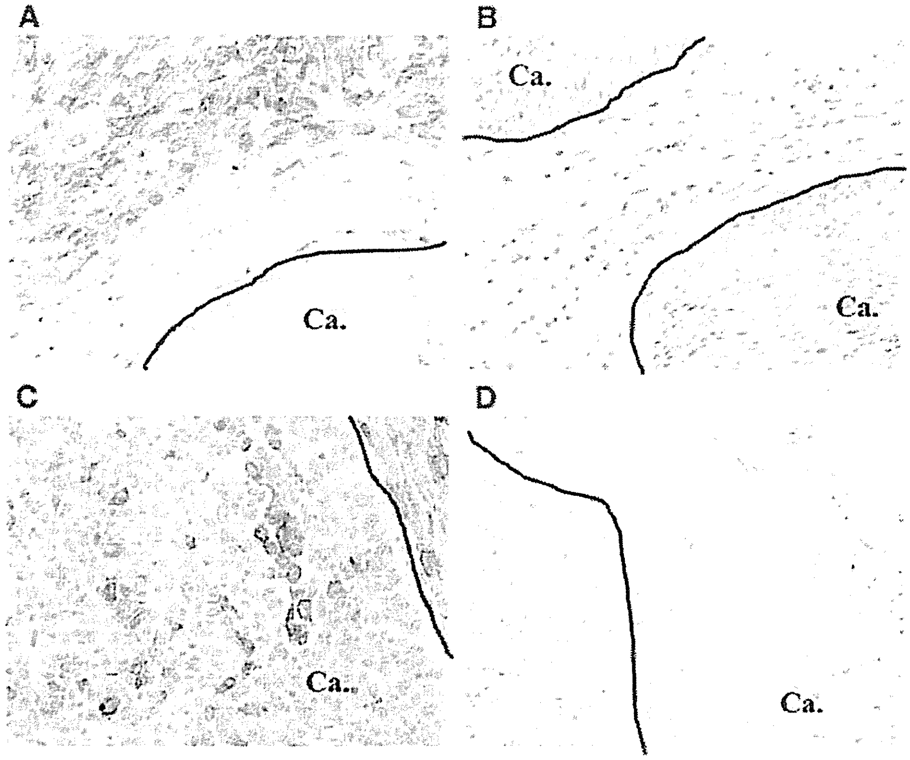

FIGURE 1. *A*, Immunohistochemical staining of squamous cell carcinoma with antihuman CD204 antibody for tumor-associated macrophages in the stroma and nest. Cases with a high number of CD204 (+) TAMs in the stroma, and *B*, a low number of CD204 (+) TAMs in the stroma. *C*, Cases with a high number of CD204 (+) TAMs in the nest, and *D*, a low number of CD204 (+) TAMs in the nest. TAMs, tumor-associated macrophages.

were compared using the log-rank test. A p value less than 0.05 was considered significant. Statistical analysis software (SPSS, version II) was used to perform the analyses.

RESULTS

Correlations between the numbers of CD204 (+) TAMs in the cancer stroma and nest and clinicopathological factors.

A representative case of immunohistochemical staining results for CD204 is shown in Fig. 1. All the patients were classified into two groups according to the median values: 30 for the stroma, and nine for the nest. A high CD204 (+) TAM count in the stroma was significantly correlated with the pathologic stage, pathologic T status, pathologic nodal involvement, and vascular and pleural invasion (Table 1). However, lymphatic permeation was significantly less frequent in the group with a high CD204 (+) TAM count in the nest, compared with those with a low CD204 (+) TAM count in the nest (Supplemental Table 2, Supplemental Digital Content 2, http://links.lww.com/JTO/A348).

Evaluation of CD204 (+) TAMs in Stroma and Nest as Prognostic Factors

The OS and RFS were significantly shorter in the group with a high CD204 (+) TAM count in the stroma compared with the group with a low CD204 (+) TAM count in the stroma, for all stages (p = 0.0005 and p = 0.0002, respectively) (Fig. 2A). In the p-stage I patients, the OS and RFS were also significantly shorter in the group with a high CD204 (+) TAM count in the stroma, compared with the group with a low CD204 (+) TAM count in the stroma (p = 0.0154 and p = 0.0071) (Fig. 2*B*). A high CD204 (+) TAM count in the stroma was marginally related to the OS and RFS among the p-stage II patients (Fig. 2*C*), but no significant relation with prognosis was seen among the p-stage III patients (Fig. 2*D*). In contrast, no relationship was seen between a high CD204 (+) TAM count in the nest and the prognosis (data not shown).

Correlations among the numbers of CD204 (+) TAMs in the stroma, Foxp3-positive lymphocytes, and the microvessel density Recent studies showed that CD204 (+) TAMs contribute to the development of neovascularization and immunesuppression. We examined the numbers of Foxp3 (+) lymphocytes (regulatory T cells) and the MVD in all the cases (Fig. 3A–D). The numbers of CD204 (+) TAMs in the stroma were strongly correlated with the MVD ($p < 0.001$; $r_s = 0.471$) and were moderately correlated with the numbers of Foxp3-positive lymphocytes (p = 0.034; $r_s = 0.147$) (Fig. 3*E* and *F*).

Correlations between the numbers of CD204 (+) TAMs in the stroma and cytokine expression in the cancer tissues. We examined the expressions of factors involved in the recruitment of TAMs, regulatory T cells, and endothelial cells. The correlations between MVD monocyte chemoattractant protein-1 (MCP-1), IL-10, transforming growth factor β, and vascular endothelial growth factor (VEGF) expression and the numbers of CD204 (+) TAMs in the tumor tissue specimens (n = 13) were analyzed. The ratios of MCP-1 expression in the cancer tissues to their levels of expression in noncancerous tissues were significantly higher in the CD204 high group (p = 0.032) (Fig. 4A). The ratios of IL-10 and transforming growth factor β expressions in the cancer tissues to their levels of expression in noncancerous tissue were marginal higher in the CD204 high group (p = 0.063 and p = 0.086,

TABLE 1. Relationship between CD204 (+) Tumor-Associated Macrophages in Stroma and Clinical Features

Variables	CD204 Low (n = 93)	CD204 High (n = 115)	p^a
Sex			
Male	85	103	
Female	8	12	0.6556
Age (yr)			
<70	49	63	
70≤	44	52	0.7632
Smoking history			
Never smoker	3	10	
Smoker	90	105	0.1052
Surgical procedures			
Lobectomy + segmentectomy	82	94	
Pneumonectomy	11	21	0.2475
Pathological stage			
Stage I	56	48	
Stage II–IIIA	37	67	0.0081[b]
T states			
T1	34	24	
T2–4	59	91	0.0121[b]
Lymph node metastasis			
N(−)	65	60	
N(+)	28	55	0.0095[b]
Vascular invasion			
V(−)	37	28	
V(+)	56	87	0.0169[b]
Lymphatic permeation			
Ly(−)	71	87	
Ly(+)	22	28	0.9076
Pleural invasion			
P(−)	66	68	
P(+)	27	47	0.018[b]

[a]Pearson 2 test.
[b]p <0.05.

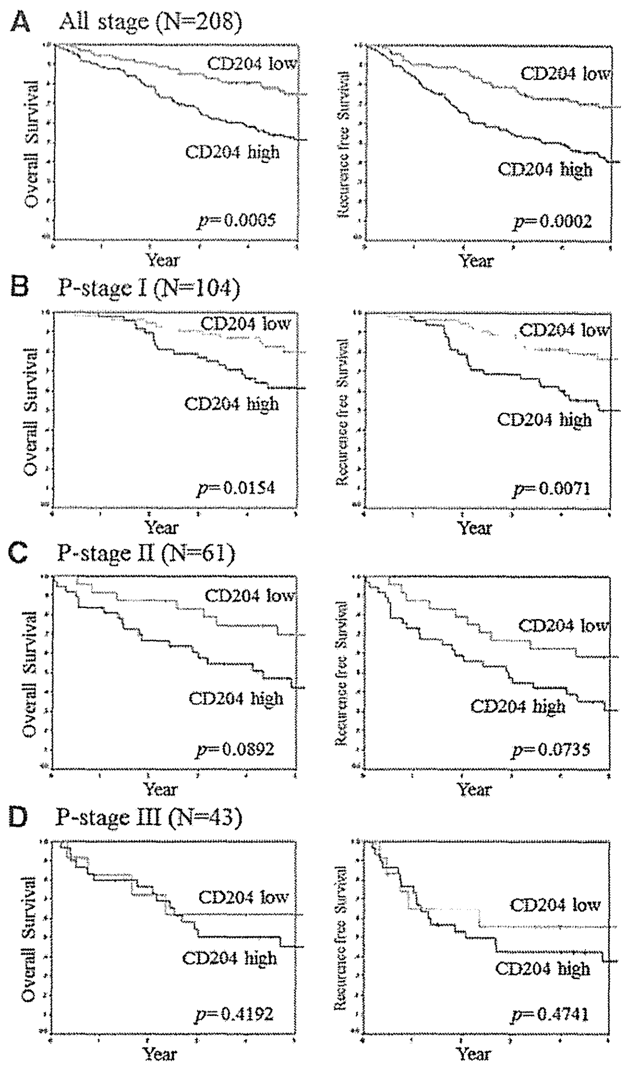

FIGURE 2. Kaplan–Meier analysis stratified according to a high or low number of CD204 (+) TAMs in the stroma. The Kaplan–Meier analysis for overall survival and recurrence-free survival according to the numbers of CD204 (+) TAMs in the stroma are shown for all stages *A*, for p-stage I, *B*, for p-stage II, *C*, and for p-stage III, *D*,. TAMs, tumor-associated macrophages.

respectively) (Fig. 4*B*, *C*). The difference in the expression of VEGF between the two groups was not significant (Fig. 4*D*).

Univariate and Multivariate Analyses of Factors Associated with Prognosis

A univariate analysis identified four significant risk factors for OS: CD204 (+) TAMs in the stroma, p-T status, vessel invasion, and pleural invasion (Table 2). In a multivariate analysis, the presence of CD204 (+) TAMs and the p-T status were shown to be statistically significant independent predictors of the OS (Table 3).

DISCUSSION

In this study, we first showed that the numbers of CD204 (+) TAMs in the tumor stroma, but not in the tumor nest, were correlated with several conventional prognostic factors in squamous cell carcinoma of the lung. Furthermore, we showed that the cases with higher numbers of CD204 (+) TAMs in the stroma had a poor clinical outcome, particularly in the early stages. These results were consisted with previous reports in other types of malignancies, such as glioma, ovarian epithelial tumors, pancreatic cancer, and lung adenocarcinoma.[6,9–11] Moreover, the numbers of CD204 (+) TAMs were related to the numbers of Foxp3 (+) lymphocytes and the MVD. These data suggested that in squamous cell carcinoma tissue, CD204 (+) TAMs, along with other tumor-promoting stromal cells such as regulatory T cells and endothelial cells, create a specific microenvironment that supports tumor progression.

TAMs are known to induce the proliferation, survival, and invasion of tumor cells by producing wide range

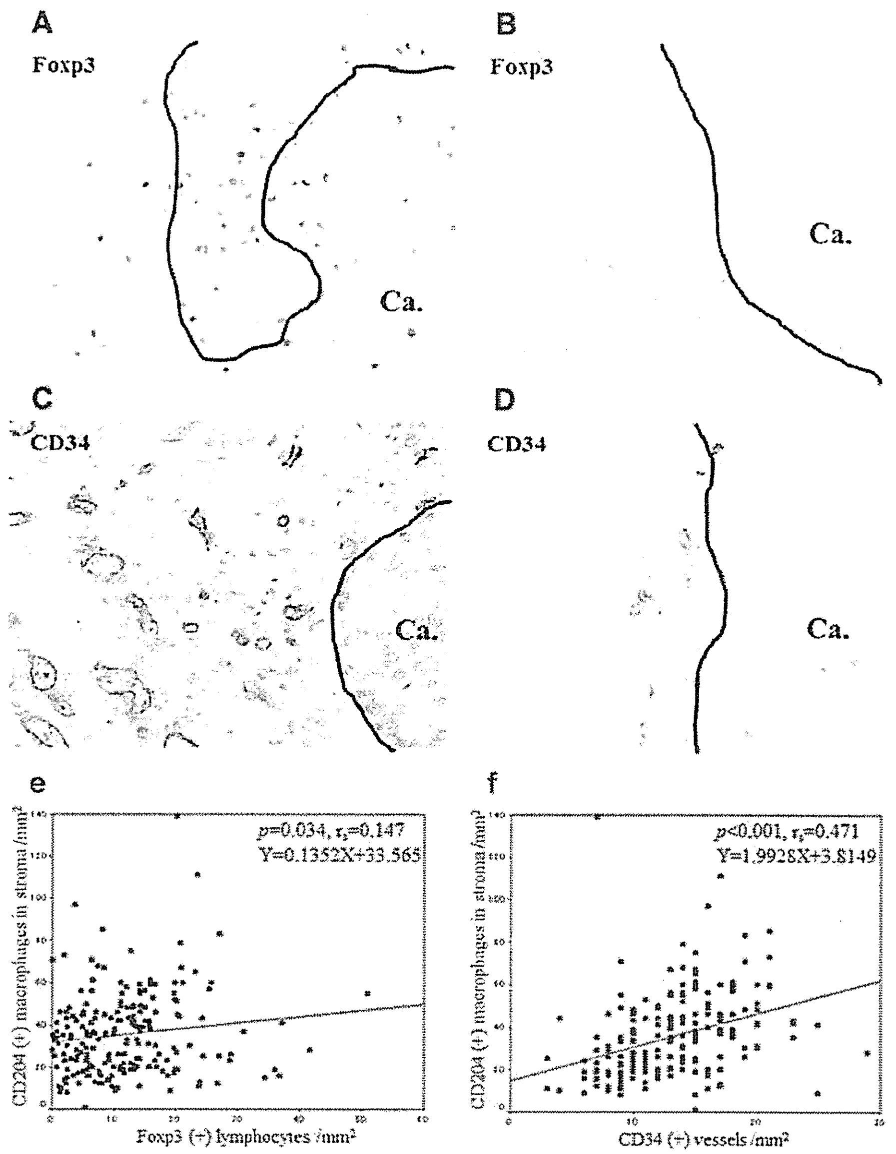

FIGURE 3. Immunohistochemical staining of squamous cell carcinoma tissue with antihuman Foxp3 antibody and antihuman CD34 antibody. *A*, Cases with a high number of Foxp3 positive lymphocytes, and *B*, a low number of Foxp3 positive lymphocytes. *C*, Cases with a high MVD, and *D*, a low MVD. *E*, Correlations between the numbers of CD204 (+) TAMs in the stroma and the MVD, *F*, the number of Foxp3 (+) lymphocytes. TAMs, tumor-associated macrophages; MVD, microvessel density.

of factors, such as matrix metalloproteinases (MMP).[1,13–16] Hagemann et al.[17] reported that TAMs change to M2 phenotype macrophages, CD204 (+) TAMs, after cocultivation with ovarian cancer cells. CD204 (+) TAMs showed a significant up-regulation of mRNA for the genes MMP−1, −2, −7, −9, and −14. Another article reported that the co-cultivation of breast cancer cells with macrophages led to the enhanced invasiveness of the cancer cells as a result of tumor necrosis factor α-dependent MMP-9 secretion from the TAMs.[18] These observations may explain the enhanced vascular and pleural invasion of squamous cell carcinoma cells in the high CD204 (+) TAMs groups in the current study.

We found that the numbers of CD204 (+) TAMs were strongly correlated with the MVD. Kawahara et al.[19] showed similar results that M2 macrophages were correlated with the MVD in gastric cancer. Given the previous report that CD204 (+) TAMs secrete proangiogenic factors, including VEGF,[17] the positive relation observed between CD204 (+) TAMs and the MVD in the present study is understandable. However, the numbers of CD204 (+) TAMs were not associated with the expression of VEGF in the tumor tissue. This discrepancy might be caused by the fact that angiogenesis also depends on angiogenic factors other than VEGF.

The number of CD204 (+) TAMs in the stroma was marginally correlated with the number of Foxp3 (+) lymphocytes, which was partly consistent with the results for intrahepatic cholangiocarcinoma.[20] Foxp3 (+) T cells down-regulate the immune response by attenuating the host's antitumor T cells, potentially permitting unrestricted growth, subsequent metastasis, and recurrence.[21,22] Taking these into consideration, CD204 (+) TAMs may not only enhance tumor cell invasiveness directly, but may also create a more tumor-promoting microenvironment by recruiting endothelial cells and regulatory T cells.

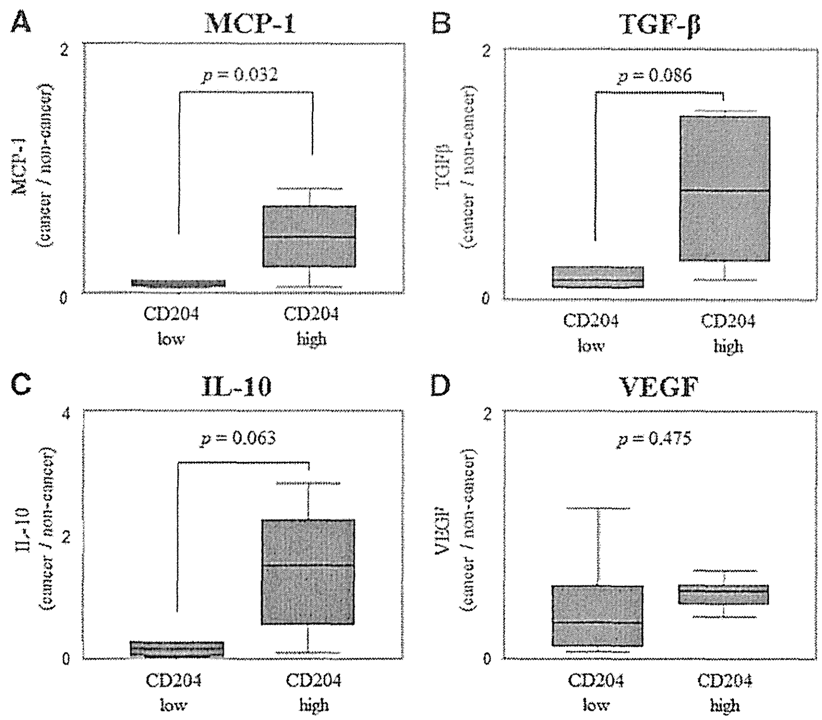

FIGURE 4. Relative mRNA expression in CD204-low and CD204-high cases. The levels of mRNA expression shown are the ratios of expression in cancer tissues relative to the expression in noncancerous tissues, as determined using a quantitative real-time polymerase chain reaction. MCP-1, monocyte chemoattractant protein-1; TGF β, transforming growth factor β; VEGF, vascular endothelial growth factor; IL-10, interleukins-10.

TABLE 2. Univariate Analysis for Overall Survival (N =208)

Variables	Category	All Cases	5-Year Survival (%)	p^a
Age				
Median, yrs (range)	69 (46–88)			0.1436
	<70	112	66	
	≥70	96	58	
Sex	Female	20	48	0.3689
	Male	188	63	
Smoking	Never	13	35	0.1894
	Ever	195	64	
Surgical procedures	Lobectomy segmentectomy	176	63	0.2908
	Pneumonectomy	32	56	
T factor	≤T1	58	84	0.0006[b]
	>T1	150	54	
N factor	pN0	125	66	0.1891
	pN1/pN2	83	56	
Lymphatic permeation	Absent	158	61	0.4973
	Present	50	67	
Vascular invasion	Absent	65	73	0.0381[b]
	Present	143	57	
Pleural invasion	Absent	134	70	0.0013[b]
	Present	74	47	
CD204 (+) TAMs in stroma	Low	93	75	0.0005[b]
	High	115	52	
CD204 (+) TAMs in nest	Low	91	63	0.5894
	High	117	61	

[a]Log-rank test.
[b]p 0.05.
TAMs, tumor-associated macrophages.

TABLE 3. Multivariate Analysis for Overall survival

Variables	Favorable	Unfavorable	Overall Survival Hazard Ratio	95% Confidence Interval	*p*
T factor	≤T1	>T1	0.486	0.246–0.957	0.037
Vascular invasion	Absent	Present	1.124	0.650–1.942	0.676
Pleural invasion	Absent	Present	1.447	0.895–2.340	0.132
CD204 (+) TAMs in stroma	Low	High	2.053	1.273–3.311	0.003

TAMs, tumor-associated macrophages.

In the present study, we showed that the tissue expression of MCP-1 was significantly correlated with the numbers of CD204 (+) TAMs. MCP-1 has been reported as a key cytokine that induces the migration, accumulation, and differentiation of the M2 phenotype and contributes to the recruitment of CD204 (+) TAMs into the tumor tissue.[11,23] Moreover, MCP-1 can act directly on endothelial cells to promote angiogenesis.[24] Although no significant association was seen between the number of CD204 (+) TAMs and the VEGF mRNA level, MCP-1 might contribute to an increase in the MVD.

In this study, there 10 patients received postoperative adjuvant chemotherapy and 21 patients received chemotherapy after recurrence. However, there are no differences in the prognosis with or without postoperative adjuvant chemotherapy (RFS; $p = 0.2329$, OS; $p = 0.2548$) and chemotherapy after recurrence (OS; $p = 0.1318$). Among 198 patients who did not receive adjuvant chemotherapy, a high number of CD204 (+) TAMs in the stroma was also a significant prognostic factor for all *p*-stages and *p*-stage I (All p-stages: RFS $p = 0.0002$, OS $p = 0.0012$, *p*-stageI: RFS $p = 0.0169$, OS $p = 0.0369$). Therefore CD204-positive TAM was a strongly independent prognostic factor, even subtracting the effect of treatment.

In a recent report, the actions of bisphosphonates on macrophages not only impaired TAMs recruitment, but also inhibited the release of proangiogenic factors capable of affecting TAMs by reversing their polarization from the M2 to the M1 phenotype.[25] Moreover, the depletion of TAMs by clodrolip, which consists of a liposome encapsulating clodronate or zoledronic acid in combination with sorafenib, significantly inhibited tumor progression in hepatocellular carcinoma in vitro.[26] Our current results suggest that the targeting of CD204 (+) TAMs may be useful as a supplemental therapy for conventional cancer-treatment regimens for lung squamous cell carcinoma.

ACKNOWLEDGMENTS

This work was supported by the Grant-in-Aid for Cancer Research (19-10) from the Ministry of Health, Labour, and Welfare, the Foundation for the Promotion of Cancer Research, 3rd-Term Comprehensive 10-Year Strategy for Cancer Control, Program for the Promotion of Fundamental Studies in Health Sciences of the National Institute of Biomedical Innovation, National Cancer Center Research and Development Fund and Japan Society for the Promotion of Science (JSPS) KAKENHI (20590417, 215981).

REFERENCES

1. Mantovani A, Allavena P, Sica A, Balkwill F. Cancer-related inflammation. *Nature* 2008;454:436–444.
2. Balkwill F, Mantovani A. Inflammation and cancer: back to Virchow? *Lancet* 2001;357:539–545.
3. Bingle L, Brown NJ, Lewis CE. The role of tumour-associated macrophages in tumour progression: implications for new anticancer therapies. *J Pathol* 2002:196:254–265.
4. Pollard JW. Tumour-educated macrophages promote tumour progression and metastasis. *Nat Rev Cancer* 2004;4:71–78.
5. Mantovani A, Sica A, Sozzani S, Allavena P, Vecchi A, Locati M. The chemokine system in diverse forms of macrophage activation and polarization. *Trends Immunol* 2004;25:677–686.
6. Komohara Y, Ohnishi K, Kuratsu J, Takeya M. Possible involvement of the M2 anti-inflammatory macrophage phenotype in growth of human gliomas. *J Pathol* 2008;216:15–24.
7. Kawamura K, Komohara Y, Takaishi K, Katabuchi H, Takeya M. Detection of M2 macrophages and colony-stimulating factor 1 expression in serous and mucinous ovarian epithelial tumors. *Pathol Int* 2009;59:300–305.
8. Allavena P, Sica A, Solinas G, Porta C, Mantovani A. The inflammatory micro-environment in tumor progression: the role of tumor-associated macrophages. *Crit Rev Oncol Hematol* 2008;66:1–9.
9. Bak SP, Walters JJ, Takeya M, Conejo-Garcia JR, Berwin BL. Scavenger receptor-A-targeted leukocyte depletion inhibits peritoneal ovarian tumor progression. *Cancer Res* 2007;67:4783–4789.
10. Kurahara H, Shinchi H, Mataki Y, et al. Significance of M2-polarized tumor-associated macrophage in pancreatic cancer. *J Surg Res* 2011;167: e211–e219.
11. Ohtaki Y, Ishii G, Nagai K, et al. Stromal macrophage expressing CD204 is associated with tumor aggressiveness in lung adenocarcinoma. *J Thorac Oncol* 2010;5:1507–1515.
12. Luo Y, Zhou H, Krueger J, et al. Targeting tumor-associated macrophages as a novel strategy against breast cancer. *J Clin Invest* 2006;116:2132–2141.
13. Giraudo E, Inoue M, Hanahan D. An amino-bisphosphonate targets MMP-9-expressing macrophages and angiogenesis to impair cervical carcinogenesis. *J Clin Invest* 2004;114:623–633.
14. Qian BZ, Pollard JW. Macrophage diversity enhances tumor progression and metastasis. *Cell* 2010;141:39–51.
15. Wyckoff J, Wang W, Lin EY, et al. A paracrine loop between tumor cells and macrophages is required for tumor cell migration in mammary tumors. *Cancer Res* 2004;64:7022–7029.
16. Fujiwara Y, Komohara Y, Ikeda T, Takeya M. Corosolic acid inhibits glioblastoma cell proliferation by suppressing the activation of signal transducer and activator of transcription-3 and nuclear factor-kappa B in tumor cells and tumor-associated macrophages. *Cancer Sci* 2011;102: 206–211.
17. Hagemann T, Wilson J, Burke F, et al. Ovarian cancer cells polarize macrophages toward a tumor-associated phenotype. *J Immunol* 2006;176:5023–5032.
18. Hagemann T, Robinson SC, Schulz M, Trümper L, Balkwill FR, Binder C. Enhanced invasiveness of breast cancer cell lines upon co-cultivation with macrophages is due to TNF-alpha dependent up-regulation of matrix metalloproteases. *Carcinogenesis* 2004;25:1543–1549.
19. Kawahara A, Hattori S, Akiba J, et al. Infiltration of thymidine phosphorylase-positive macrophages is closely associated with tumor

angiogenesis and survival in intestinal type gastric cancer. *Oncol Rep* 2010;24:405–415.
20. Hasita H, Komohara Y, Okabe H, et al. Significance of alternatively activated macrophages in patients with intrahepatic cholangiocarcinoma. *Cancer Sci* 2010;101:1913–1919.
21. Petersen RP, Campa MJ, Sperlazza J, et al. Tumor infiltrating Foxp3+ regulatory T-cells are associated with recurrence in pathologic stage I NSCLC patients. *Cancer* 2006;107:2866–2872.
22. Shimizu K, Nakata M, Hirami Y, Yukawa T, Maeda A, Tanemoto K. Tumor-infiltrating Foxp3+ regulatory T cells are correlated with cyclooxygenase-2 expression and are associated with recurrence in resected non-small cell lung cancer. *J Thorac Oncol* 2010;5:585–590.
23. Fujimoto H, Sangai T, Ishii G, et al. Stromal MCP-1 in mammary tumors induces tumor-associated macrophage infiltration and contributes to tumor progression. *Int J Cancer* 2009;125:1276–1284.
24. Salcedo R, Ponce ML, Young HA, et al. Human endothelial cells express CCR2 and respond to MCP-1: direct role of MCP-1 in angiogenesis and tumor progression. *Blood* 2000;96:34–40.
25. Rogers TL, Holen I. Tumour macrophages as potential targets of bisphosphonates. *J Transl Med* 2011;9:177.
26. Zhang W, Zhu XD, Sun HC, et al. Depletion of tumor-associated macrophages enhances the effect of sorafenib in metastatic liver cancer models by antimetastatic and antiangiogenic effects. *Clin Cancer Res* 2010;16:3420–3430.

BJC OPEN

British Journal of Cancer (2012), 1–5

www.bjcancer.com

Full Paper

KRAS mutations in primary tumours and post-FOLFOX metastatic lesions in cases of colorectal cancer

Y Kawamoto[1,2,3,4], K Tsuchihara*[,2], T Yoshino[3], N Ogasawara[2], M Kojima[5], M Takahashi[3], A Ochiai[5], H Bando[3], N Fuse[3], M Tahara[3], T Doi[3], H Esumi[2], Y Komatsu[4] and A Ohtsu[3]

[1]*Department of Gastroenterology, Hokkaido University Graduate School of Medicine, Sapporo 060-8638, Japan;* [2]*Cancer Physiology Project, Research Center for Innovative Oncology, National Cancer Center Hospital East, Kashiwa 277-8577, Japan;* [3]*Department of Gastroenterology and Gastrointestinal Oncology, National Cancer Center Hospital East, Kashiwa 277-8577, Japan;* [4]*Department of Cancer Center, Hokkaido University Hospital, Sapporo 060-8638, Japan;* [5]*Pathology Division, Research Center for Innovative Oncology, National Cancer Center Hospital East, Kashiwa 277-8577, Japan*

BACKGROUND: *KRAS* mutations are predictive markers for the efficacy of anti-EGFR antibody therapies in patients with metastatic colorectal cancer. Although the mutational status of *KRAS* is reportedly highly concordant between primary and metastatic lesions, it is not yet clear whether genotoxic chemotherapies might induce additional mutations.

METHODS: A total of 63 lesions (23 baseline primary, 18 metastatic and 24 post-treatment metastatic) from 21 patients who were treated with FOLFOX as adjuvant therapy for stage III/IV colorectal cancer following curative resection were examined. The DNA samples were obtained from formalin-fixed paraffin-embedded specimens, and *KRAS, NRAS, BRAF* and *PIK3CA* mutations were evaluated.

RESULTS: The numbers of primary lesions with wild-type and mutant *KRAS* codons 12 and 13 were 8 and 13, respectively. The mutational status of *KRAS* remained concordant between the primary tumours and the post-FOLFOX metastatic lesions, irrespective of patient background, treatment duration and disease-free survival. Furthermore, the mutational statuses of the other genes evaluated were also concordant between the primary and metastatic lesions.

CONCLUSION: Because the mutational statuses of predictive biomarker genes were not altered by FOLFOX therapy, specimens from both primary tumours and post-FOLFOX tumour metastases might serve as valid sources of DNA for known genomic biomarker testing.

British Journal of Cancer advance online publication, 22 May 2012; doi:10.1038/bjc.2012.218 www.bjcancer.com

Keywords: colorectal cancer; genomic biomarker; *KRAS*; anti-EGFR antibody; oxaliplatin

KRAS mutations are predictive markers for the poor efficacy of anti-EGFR antibody therapies in patients with metastatic colorectal cancer (Lievre *et al*, 2006; Benvenuti *et al*, 2007; Di Fiore *et al*, 2007; Frattini *et al*, 2007; Khambata-Ford *et al*, 2007; Amado *et al*, 2008; De Roock *et al*, 2008; Freeman *et al*, 2008; Karapetis *et al*, 2008; Lievre *et al*, 2008). Point mutations in the *KRAS* gene occur early in the progression from colorectal adenoma to carcinoma and are detected in 35–40% of patients, regardless of their Dukes stage (Andreyev *et al*, 1998). More than 90% of the *KRAS* mutations in these patients have been detected in codons 12 (GGT) and 13 (GGC) (Oliveira *et al*, 2004). Activating mutations at codons 61 and 146 have also been reported in a small number of these tumours. In addition, mutations in the molecules involved in signalling pathways downstream of EGFR, such as *NRAS, BRAF* and *PIK3CA*, have also been reported in colorectal cancers. These mutations have been suggested to modify the efficacy of anti-EGFR antibody therapies, although their predictive value has not yet been established (De Roock *et al*, 2010).

Oxaliplatin [*trans*-R,R-1,2-diaminocyclohexaneoxalatoplatinum (II), L-OHP] is a third-generation platinum (Pt)-containing anti-tumour compound. It is frequently administered as a component of FOLFOX therapy in combination with 5-FU for patients with metastatic colorectal cancer. Oxaliplatin induces DNA damage associated with intra- and inter-strand cross-links (Pt-GG adducts) and can induce gene mutations (Woynarowski *et al*, 2000; Hah *et al*, 2007; Sharma *et al*, 2007). The mutagenic activity of oxaliplatin has been demonstrated in cultured cells (Silva *et al*, 2005).

The *KRAS* mutation status of primary and metastatic lesions is reportedly highly concordant (Oudejans *et al*, 1991; Losi *et al*, 1992; Suchy *et al*, 1992; Zauber *et al*, 2003; Weber *et al*, 2007; Etienne-Grimaldi *et al*, 2008; Santini *et al*, 2008; Garm Spindler *et al*, 2009; Loupakis *et al*, 2009; Perrone *et al*, 2009; Baldus *et al*, 2010; Italiano *et al*, 2010; Knijn *et al*, 2011). However, whether long-term treatment with genotoxic chemotherapies, such as oxaliplatin, can induce additional mutations in metachronous metastatic lesions has not yet been well examined.

Assuming that FOLFOX therapy has the potential to alter the biomarker mutation profile, it is important to determine whether

*Correspondence: Dr K Tsuchihara; E-mail: ktsuchih@east.ncc.go.jp
Received 14 February 2012; revised 25 April 2012; accepted 29 April 2012

the primary or relapsed tumour represents the more appropriate source of DNA for testing. We examined the mutation status of *KRAS* and other biomarker genes in primary and synchronous/metachronous metastatic lesions in patients with stage III/IV colorectal cancer treated with adjuvant FOLFOX therapy following curative resection.

PATIENTS AND METHODS

Patient selection

A total of 63 lesions from 21 patients who had received adjuvant FOLFOX therapy for stage III/IV colorectal cancer following curative resection at the National Cancer Center Hospital East, Japan, between January 2006 and December 2009 were examined.

All patients were treated with a modified FOLFOX6 regimen, with a reduced oxaliplatin dose of 85 mg m^{-2} administered every 14 days, and 12 cycles were planned as the full therapy course (Andre *et al*, 2004; Allegra *et al*, 2009). FOLFOX therapy was discontinued when tumour relapse was demonstrated by imaging or when intolerable adverse events occurred.

DNA samples and mutational analyses

The DNA samples were obtained from macroscopically dissected formalin-fixed paraffin-embedded specimens cut into 10-μm-thick sections. Genomic DNA was extracted using the EZ1 Advanced XL and EZ1 DNA Tissue Kits (Qiagen, Hilden, Germany) according to the manufacturer's instructions (Bando *et al*, 2011). Mutations in *KRAS* codons 12 and 13 were detected using the ARMS/Scorpions technology-based *KRAS* PCR Kit (Qiagen) according to the manufacturer's instructions. Mutations in *KRAS* codons 61 and 146, *NRAS* codons 12, 13 and 61, *BRAF* codon 600 and *PIK3CA* codons 542, 545, 546 and 1047 were detected using the multiplex PCR-Luminex method-based MEBGEN Mutation Kit (Medical & Biological Laboratories, Nagoya, Japan). Mutations detected with the MEBGEN Mutation Kit were confirmed by direct sequencing. Mutations in *PIK3CA* codons 542, 545 and 546 were further confirmed using the ARMS/Scorpions technology-based PI3K Mutation Test Kit (Qiagen). The study was approved by the Institutional Review Board of the National Cancer Center.

RESULTS

Patient and tumour site characteristics

We reviewed 151 consecutive cases of stage III/IV colorectal cancer treated with an adjuvant FOLFOX therapy after curative resection. Among these cases, 21 patients developed metastatic tumours that were diagnosed during or after the FOLFOX therapy and surgically resected. The patient and tumour site characteristics are shown in Table 1. The primary tumour sites were the colon and rectum in 8 and 13 patients, respectively. The most abundant primary tumour histopathological type was differentiated adenocarcinoma. Well- and moderately differentiated adenocarcinomas and mucinous adenocarcinomas were observed in 5, 14 and 2 patients, respectively. All metastatic tumours exhibited histology concordant with that of the associated primary colorectal adenocarcinoma.

In all, 12 patients had stage III disease, whereas the remaining 9 patients had synchronous metastatic lesions and were diagnosed as stage IV at the initial operation. There were 12 synchronous metastatic lesions in the patients with stage IV disease. In addition, six metastatic lesions were detected in five patients with stage III disease at operation that were resected prior to the start of FOLFOX therapy. These 18 lesions were regarded as 'pre-FOLFOX' metastatic lesions. The pre-FOLFOX metastases were found in the liver (11 lesions), lung (5 lesions), as a local recurrence (1 lesion) and as a subcutaneous recurrence (1 lesion). Meanwhile, 24 metastatic lesions in the 21 patients were detected during or after FOLFOX therapy. These lesions were regarded as 'post-FOLFOX' metastatic lesions. The post-FOLFOX metastases were found in the liver, lung, as a local recurrence and lymph node in 6, 14, 3 and 1 patients, respectively.

The median number of FOLFOX therapy cycles administered was 9 (3–12 cycles). Five patients experienced relapse during FOLFOX therapy (case 1, 2, 3, 7 and 12), whereas the remaining 16 patients experienced relapse after the end of FOLFOX therapy. The median disease-free survival, calculated from the time of the last operation until post-FOLFOX recurrence, was 409 days (97–1077). The median period from the start of FOLFOX therapy until recurrence was 373 days (35–1029). Relapses developed within 180 days after the end of FOLFOX therapy in 10 of the 21 patients (Table 2).

Table 1 Characteristics

Patient characteristics	Number
Sex (female/male)	8/13
Median age (range)	64 (36–75) years
Primary tumour site	
Colon	8
Rectum	13
Histopathological type of primary site	
Well-differentiated adenocarcinoma	5
Moderately differentiated adenocarcinoma	14
Mucinous adenocarcinoma	2
Stage before initial operation	
III	12
IV (synchronous metastases)	9
Tumour site characteristics	
Metastases	
Pre-FOLFOX	18
Synchronous	12
Metachronous	6
Post-FOLFOX	24
Sites of metastases	
Pre-FOLFOX	
Liver	11
Lung	5
Local recurrence	1
Subcutaneous	1
Post-FOLFOX	
Liver	6
Lung	14
Local recurrence	3
Lymph node	1

Mutational status of *KRAS* and other genes

The mutational statuses of *KRAS* and other genes in primary and metastatic lesions are shown in Table 3. Mutations in *KRAS* codons 12 and 13 were detected in 13 of the 21 primary colorectal tumours. Among the remaining eight tumours with wild-type *KRAS* codons 12 and 13, two tumours exhibited *KRAS* codon 146 mutations (A146V and A146T) and one tumour exhibited *NRAS* codon 61 mutation (Q61H). Two tumours exhibited mutations in *PIK3CA* codon 542 (E542K), one tumour exhibited a *KRAS* G12S mutation and one tumour had no mutations in any of the genes examined. No apparent mutations of *KRAS* codon 61, *NRAS* codon

Table 2 FOLFOX treatment, metastasis status and tumour recurrence sites

Case	Primary site	Histopathological type	Pre-FOLFOX metastatic site	Synchronous/ metachronous	FOLFOX cycles	DFS (days)	Days from end of FOFLOX until recurrence	Post-FOLFOX recurrence site
1	Rectum	Mode		—	3	124	6	Liver
2	Colon	Mode	Liver	Synchronous	4	97	−16[a]	Liver
3	Colon	Mode	Liver	Synchronous	4	116	26	Liver
4	Rectum	Well	Local recurrence	Metachronous	4	469	363	Local recurrence
5	Rectum	Mode	—	—	5	827	603	Lung
6	Colon	Mode	—	—	5	350	244	Lymph node
7	Rectum	Mode	Liver	Synchronous	8	214	1	Lung
			Lung	Synchronous				
8	Rectum	Muc	—	—	8	538	318	Lung
9	Colon	Well	—	—	8	1077	903	Liver
10	Colon	Mode	Liver	Synchronous	8	344	120	Lung
			Liver	Synchronous				Lung
			Lung	Synchronous				
11	Colon	Muc	Lung	Synchronous	9	721	401	Lung
12	Rectum	Well	Liver	Synchronous	9	109	−88[a]	Liver
13	Rectum	Mode	Liver	Metachronous	11	328	120	Liver
			Lung	Metachronous				
14	Rectum	Mode	Subcutaneous	Metachronous	12	519	156	Lung
15	Colon	Mode	—	—	12	388	176	Local recurrence
16	Rectum	Mode	Liver	Synchronous	12	466	210	Lung
17	Rectum	Well	Lung	Synchronous	12	556	264	Lung
18	Colon	Mode	Liver	Metachronous	12	531	231	Lung
								Lung
19	Rectum	Mode	Liver	Synchronous	12	409	217	Lung
20	Rectum	Mode	—	—	12	455	243	Local recurrence
21	Rectum	Well	Liver	Metachronous	12	346	71	Lung
								Lung

Abbreviations: DFS = disease-free survival; mode = moderately differentiated adenocarcinoma; muc = mucinous adenocarcinoma; well = well-differentiated adenocarcinoma.
[a]The cases that FOLFOX therapies were administered after recurrence.

Table 3 Mutational status of *KRAS* and other genes

Case	Primary site	Mutation status	Pre-FOLFOX metastatic site	Mutation status	Post-FOLFOX recurrence site	Mutation status
1	Rectum	KRAS G12D	—	—	Liver	KRAS G12D
2	Colon	KRAS G12D	Liver	KRAS G12D	Liver	KRAS G12D
3	Colon	KRAS G12D	Liver	KRAS G12D	Liver	KRAS G12D
4	Rectum	KRAS G12R	Local recurrence	KRAS G12R	Local recurrence	KRAS G12R
5	Rectum	KRAS G12D	—		Lung	KRAS G12D
6	Colon	WT	—		LN	WT
7	Rectum	KRAS G12S	Liver	KRAS G12S	Lung	KRAS G12S
			Lung	KRAS G12S		
8	Rectum	WT	—	—	Lung	WT
9	Colon	WT	—		Liver	WT
10	Colon	KRAS G12A	Liver	KRAS G12A	Lung	KRAS G12A
			Liver	KRAS G12A	Lung	KRAS G12A
			Lung	WT		
11	Colon	KRAS G13D	Lung	KRAS G13D	Lung	KRAS G13D
12	Rectum	KRAS A146V	Liver	KRAS A146V	Liver	KRAS A146V
13	Rectum	KRAS G12V	Liver	KRAS G12V	Liver	KRAS G12V
			Lung	KRAS G12V		
14	Rectum	KRAS G12D	Subcutaneous	KRAS G12D	Lung	KRAS G12D
15	Colon	WT	—	—	Local recurrence	WT
16	Rectum	KRAS G12S, PIK3CA E542K	Liver	KRAS G12S, PIK3CA E542K	Lung	KRAS G12S, PIK3CA E542K
17	Rectum	KRAS G12D	Lung	KRAS G12D	Lung	KRAS G12D
18	Colon	KRAS G12D	Liver	KRAS G12D	Lung	KRAS G12D
					Lung	KRAS G12D
19	Rectum	NRAS Q61H	Liver	NRAS Q61H	Lung	NRAS Q61H
20	Rectum	PIK3CA E542K	—		Local recurrence	PIK3CA E542K
21	Rectum	KRAS A146V	Liver	KRAS A146V	Lung	KRAS A146V
					Lung	KRAS A146V

Abbreviations: LN = lymph node; WT = wild-type.

12 or 13, *BRAF* codon 600, or *PIK3CA* codon 1047 were detected in any sample in this study.

The degree of concordance of the gene mutations in primary and pre-FOLFOX metastatic lesions was examined. In case 10, a *KRAS* G12A mutation was detected in the primary lesion, whereas the metastatic lesion in the lung had wild-type *KRAS*. Although the histological features of the lung lesion were consistent with metastatic adenocarcinoma of the colon, no mutations in the metastatic lesion were detected, even after repeated high-sensitivity examinations. The remaining 17 metastatic lesions in 14 patients, including 2 liver metastatic lesions in case 10, showed the same mutational statuses as the primary tumours for all of the genes examined.

Then, the mutational statuses of the post-FOLFOX metastatic lesions were examined. The mutational statuses of all genes examined were identical in the 21 primary tumours and the corresponding 24 post-FOLFOX metastatic lesions, regardless of the sites involved, duration of FOLFOX treatment or disease-free survival period.

DISCUSSION

Previous studies have reported a high concordance rate of the *KRAS* mutations in primary and metastatic tumours (Oudejans *et al*, 1991; Losi *et al*, 1992; Suchy *et al*, 1992; Zauber *et al*, 2003; Weber *et al*, 2007; Etienne-Grimaldi *et al*, 2008; Santini *et al*, 2008; Garm Spindler *et al*, 2009; Loupakis *et al*, 2009; Perrone *et al*, 2009; Baldus *et al*, 2010; Italiano *et al*, 2010; Knijn *et al*, 2011). However, in patients receiving long-term chemotherapy, the effects of genotoxic chemotherapies, such as oxaliplatin, have not been well investigated.

In this study, we examined 21 patients with metastatic colorectal cancer who received adjuvant FOLFOX therapy. The recurrent tumours in three patients who showed relapse within 4 months after the primary surgery or during the first 3 or 4 cycles of adjuvant FOLFOX therapy (cases 1–3) were regarded as synchronous metastases arising from micrometastases that likely existed prior to the start of the adjuvant chemotherapy. The remaining 18 patients who developed relapses more than 8 months from the end of adjuvant FOLFOX therapy or after more than 6 cycles of adjuvant FOLFOX therapy were regarded as having metachronous metastatic tumours that had developed after exposure to oxaliplatin. Among these cases, tumour relapse occurred within 180 days after FOLFOX therapy in 7 patients and more than 180 days after FOLFOX therapy in the remaining 11 patients. Regardless of the treatment duration, 8 of the primary tumours with wild-type *KRAS* codons 12 and 13 did not acquire *KRAS* mutations. The remaining tumours with *KRAS* mutations also did not show additional mutations after FOLFOX therapy. Furthermore, none of the other genes that might potentially affect the efficacy of anti-EGFR antibody therapy were altered.

KRAS, *NRAS* and *BRAF* mutations are all regarded as strong driver mutations that induce cell proliferation. These mutations might be acquired in the early stages of carcinogenesis and have generally been reported as mutually exclusive (Andreyev *et al*, 1998). Consistent with this observation, the *KRAS* and *NRAS* mutations in this study were found to be mutually exclusive. In the rest of the tumours, other unidentified driver mutations or amplifications may have activated the signalling pathways promoting cell proliferation. Considering the exclusive nature of the tested mutations, the acquisition of additional driver mutations may not be advantageous to these tumour cells for clonal selection. This could be one explanation for why the mutational statuses of *KRAS* and other genes were not altered during the development of metastatic tumours.

Our findings suggest that both the primary tumours and metastatic tumours arising during or after FOLFOX therapy could be valid sources of DNA for *KRAS* testing prior to treatment with anti-EGFR antibodies, although the number of cases in this study was limited. This finding should be further confirmed in a larger number of cases. Though collecting surgically resected metastatic tumour tissues is often difficult, circulating tumour cells may be a useful alternative DNA source for highly reliable and sensitive mutation detection systems such as the ARMS/Scorpion method for further analyses.

ACKNOWLEDGEMENTS

The study was supported by the National Cancer Center Research and Development Fund, 23-A-2, awarded to KT and TY.

REFERENCES

Allegra CJ, Yothers G, O'Connell MJ, Sharif S, Colangelo LH, Lopa SH, Petrelli NJ, Goldberg RM, Atkins JN, Seay TE, Fehrenbacher L, O'Reilly S, Chu L, Azar CA, Wolmark N (2009) Initial safety report of NSABP C-08: a randomized phase III study of modified FOLFOX6 with or without bevacizumab for the adjuvant treatment of patients with stage II or III colon cancer. *J Clin Oncol* 27: 3385–3390

Amado RG, Wolf M, Peeters M, Van Cutsem E, Siena S, Freeman DJ, Juan T, Sikorski R, Suggs S, Radinsky R, Patterson SD, Chang DD (2008) Wild-type KRAS is required for panitumumab efficacy in patients with metastatic colorectal cancer. *J Clin Oncol* 26: 1626–1634

Andre T, Boni C, Mounedji-Boudiaf L, Navarro M, Tabernero J, Hickish T, Topham C, Zaninelli M, Clingan P, Bridgewater J, Tabah-Fisch I, de Gramont A (2004) Oxaliplatin, fluorouracil, and leucovorin as adjuvant treatment for colon cancer. *N Engl J Med* 350: 2343–2351

Andreyev HJ, Norman AR, Cunningham D, Oates JR, Clarke PA (1998) Kirsten ras mutations in patients with colorectal cancer: the multicenter 'RASCAL' study. *J Natl Cancer Inst* 90: 675–684

Baldus SE, Schaefer KL, Engers R, Hartleb D, Stoecklein NH, Gabbert HE (2010) Prevalence and heterogeneity of KRAS, BRAF, and PIK3CA mutations in primary colorectal adenocarcinomas and their corresponding metastases. *Clin Cancer Res* 16: 790–799

Bando H, Yoshino T, Tsuchihara K, Ogasawara N, Fuse N, Kojima T, Tahara M, Kojima M, Kaneko K, Doi T, Ochiai A, Esumi H, Ohtsu A (2011) KRAS mutations detected by the amplification refractory mutation system-Scorpion assays strongly correlate with therapeutic effect of cetuximab. *Br J Cancer* 105: 403–406

Benvenuti S, Sartore-Bianchi A, Di Nicolantonio F, Zanon C, Moroni M, Veronese S, Siena S, Bardelli A (2007) Oncogenic activation of the RAS/RAF signaling pathway impairs the response of metastatic colorectal cancers to anti-epidermal growth factor receptor antibody therapies. *Cancer Res* 67: 2643–2648

De Roock W, Claes B, Bernasconi D, De Schutter J, Biesmans B, Fountzilas G, Kalogeras KT, Kotoula V, Papamichael D, Laurent-Puig P, Penault-Llorca F, Rougier P, Vincenzi B, Santini D, Tonini G, Cappuzzo F, Frattini M, Molinari F, Saletti P, De Dosso S, Martini M, Bardelli A, Siena S, Sartore-Bianchi A, Tabernero J, Macarulla T, Di Fiore F, Gangloff AO, Ciardiello F, Pfeiffer P, Qvortrup C, Hansen TP, Van Cutsem E, Piessevaux H, Lambrechts D, Delorenzi M, Tejpar S (2010) Effects of KRAS, BRAF, NRAS, and PIK3CA mutations on the efficacy of cetuximab plus chemotherapy in chemotherapy-refractory metastatic colorectal cancer: a retrospective consortium analysis. *Lancet Oncol* 11: 753–762

De Roock W, Piessevaux H, De Schutter J, Janssens M, De Hertogh G, Personeni N, Biesmans B, Van Laethem JL, Peeters M, Humblet Y, Van Cutsem E, Tejpar S (2008) KRAS wild-type state predicts survival and is associated to early radiological response in metastatic colorectal cancer treated with cetuximab. *Ann Oncol* 19: 508–515

Di Fiore F, Blanchard F, Charbonnier F, Le Pessot F, Lamy A, Galais MP, Bastit L, Killian A, Sesboue R, Tuech JJ, Queuniet AM, Paillot B, Sabourin JC, Michot F, Michel P, Frebourg T (2007) Clinical relevance of KRAS

mutation detection in metastatic colorectal cancer treated by Cetuximab plus chemotherapy. *Br J Cancer* **96**: 1166–1169
Etienne-Grimaldi MC, Formento JL, Francoual M, Francois E, Formento P, Renee N, Laurent-Puig P, Chazal M, Benchimol D, Delpero JR, Letoublon C, Pezet D, Seitz JF, Milano G (2008) K-Ras mutations and treatment outcome in colorectal cancer patients receiving exclusive fluoropyrimidine therapy. *Clin Cancer Res* **14**: 4830–4835
Frattini M, Saletti P, Romagnani E, Martin V, Molinari F, Ghisletta M, Camponovo A, Etienne LL, Cavalli F, Mazzucchelli L (2007) PTEN loss of expression predicts cetuximab efficacy in metastatic colorectal cancer patients. *Br J Cancer* **97**: 1139–1145
Freeman DJ, Juan T, Reiner M, Hecht JR, Meropol NJ, Berlin J, Mitchell E, Sarosi I, Radinsky R, Amado RG (2008) Association of K-ras mutational status and clinical outcomes in patients with metastatic colorectal cancer receiving panitumumab alone. *Clin Colorectal Cancer* **7**: 184–190
Garm Spindler KL, Pallisgaard N, Rasmussen AA, Lindebjerg J, Andersen RF, Cruger D, Jakobsen A (2009) The importance of KRAS mutations and EGF61A > G polymorphism to the effect of cetuximab and irinotecan in metastatic colorectal cancer. *Ann Oncol* **20**: 879–884
Hah SS, Sumbad RA, de Vere White RW, Turteltaub KW, Henderson PT (2007) Characterization of oxaliplatin-DNA adduct formation in DNA and differentiation of cancer cell drug sensitivity at microdose concentrations. *Chem Res Toxicol* **20**: 1745–1751
Italiano A, Hostein I, Soubeyran I, Fabas T, Benchimol D, Evrard S, Gugenheim J, Becouarn Y, Brunet R, Fonck M, Francois E, Saint-Paul MC, Pedeutour F (2010) KRAS and BRAF mutational status in primary colorectal tumors and related metastatic sites: biological and clinical implications. *Ann Surg Oncol* **17**: 1429–1434
Karapetis CS, Khambata-Ford S, Jonker DJ, O'Callaghan CJ, Tu D, Tebbutt NC, Simes RJ, Chalchal H, Shapiro JD, Robitaille S, Price TJ, Shepherd L, Au HJ, Langer C, Moore MJ, Zalcberg JR (2008) K-ras mutations and benefit from cetuximab in advanced colorectal cancer. *N Engl J Med* **359**: 1757–1765
Khambata-Ford S, Garrett CR, Meropol NJ, Basik M, Harbison CT, Wu S, Wong TW, Huang X, Takimoto CH, Godwin AK, Tan BR, Krishnamurthi SS, Burris III HA, Poplin EA, Hidalgo M, Baselga J, Clark EA, Mauro DJ (2007) Expression of epiregulin and amphiregulin and K-ras mutation status predict disease control in metastatic colorectal cancer patients treated with cetuximab. *J Clin Oncol* **25**: 3230–3237
Knijn N, Mekenkamp LJ, Klomp M, Vink-Borger ME, Tol J, Teerenstra S, Meijer JW, Tebar M, Riemersma S, van Krieken JH, Punt CJ, Nagtegaal ID (2011) KRAS mutation analysis: a comparison between primary tumours and matched liver metastases in 305 colorectal cancer patients. *Br J Cancer* **104**(6): 1020–1026
Lievre A, Bachet JB, Boige V, Cayre A, Le Corre D, Buc E, Ychou M, Bouche O, Landi B, Louvet C, Andre T, Bibeau F, Diebold MD, Rougier P, Ducreux M, Tomasic G, Emile JF, Penault-Llorca F, Laurent-Puig P (2008) KRAS mutations as an independent prognostic factor in patients with advanced colorectal cancer treated with cetuximab. *J Clin Oncol* **26**: 374–379
Lievre A, Bachet JB, Le Corre D, Boige V, Landi B, Emile JF, Cote JF, Tomasic G, Penna C, Ducreux M, Rougier P, Penault-Llorca F, Laurent-Puig P (2006) KRAS mutation status is predictive of response to cetuximab therapy in colorectal cancer. *Cancer Res* **66**: 3992–3995
Losi L, Benhattar J, Costa J (1992) Stability of K-ras mutations throughout the natural history of human colorectal cancer. *Eur J Cancer* **28A**: 1115–1120
Loupakis F, Pollina L, Stasi I, Ruzzo A, Scartozzi M, Santini D, Masi G, Graziano F, Cremolini C, Rulli E, Canestrari E, Funel N, Schiavon G, Petrini I, Magnani M, Tonini G, Campani D, Floriani I, Cascinu S, Falcone A (2009) PTEN expression and KRAS mutations on primary tumors and metastases in the prediction of benefit from cetuximab plus irinotecan for patients with metastatic colorectal cancer. *J Clin Oncol* **27**: 2622–2629
Oliveira C, Westra JL, Arango D, Ollikainen M, Domingo E, Ferreira A, Velho S, Niessen R, Lagerstedt K, Alhopuro P, Laiho P, Veiga I, Teixeira MR, Ligtenberg M, Kleibeuker JH, Sijmons RH, Plukker JT, Imai K, Lage P, Hamelin R, Albuquerque C, Schwartz Jr S, Lindblom A, Peltomaki P, Yamamoto H, Aaltonen LA, Seruca R, Hofstra RM (2004) Distinct patterns of KRAS mutations in colorectal carcinomas according to germline mismatch repair defects and hMLH1 methylation status. *Hum Mol Genet* **13**: 2303–2311
Oudejans JJ, Slebos RJ, Zoetmulder FA, Mooi WJ, Rodenhuis S (1991) Differential activation of ras genes by point mutation in human colon cancer with metastases to either lung or liver. *Int J Cancer* **49**: 875–879
Perrone F, Lampis A, Orsenigo M, Di Bartolomeo M, Gevorgyan A, Losa M, Frattini M, Riva C, Andreola S, Bajetta E, Bertario L, Leo E, Pierotti MA, Pilotti S (2009) PI3KCA/PTEN deregulation contributes to impaired responses to cetuximab in metastatic colorectal cancer patients. *Ann Oncol* **20**: 84–90
Santini D, Loupakis F, Vincenzi B, Floriani I, Stasi I, Canestrari E, Rulli E, Maltese PE, Andreoni F, Masi G, Graziano F, Baldi GG, Salvatore L, Russo A, Perrone G, Tommasino MR, Magnani M, Falcone A, Tonini G, Ruzzo A (2008) High concordance of KRAS status between primary colorectal tumors and related metastatic sites: implications for clinical practice. *Oncologist* **13**: 1270–1275
Sharma S, Gong P, Temple B, Bhattacharyya D, Dokholyan NV, Chaney SG (2007) Molecular dynamic simulations of cisplatin- and oxaliplatin-d(GG) intrastand cross-links reveal differences in their conformational dynamics. *J Mol Biol* **373**: 1123–1140
Silva MJ, Costa P, Dias A, Valente M, Louro H, Boavida MG (2005) Comparative analysis of the mutagenic activity of oxaliplatin and cisplatin in the Hprt gene of CHO cells. *Environ Mol Mutagen* **46**: 104–115
Suchy B, Zietz C, Rabes HM (1992) K-ras point mutations in human colorectal carcinomas: relation to aneuploidy and metastasis. *Int J Cancer* **52**: 30–33
Weber JC, Meyer N, Pencreach E, Schneider A, Guerin E, Neuville A, Stemmer C, Brigand C, Bachellier P, Rohr S, Kedinger M, Meyer C, Guenot D, Oudet P, Jaeck D, Gaub MP (2007) Allelotyping analyses of synchronous primary and metastasis CIN colon cancers identified different subtypes. *Int J Cancer* **120**: 524–532
Woynarowski JM, Faivre S, Herzig MC, Arnett B, Chapman WG, Trevino AV, Raymond E, Chaney SG, Vaisman A, Varchenko M, Juniewicz PE (2000) Oxaliplatin-induced damage of cellular DNA. *Mol Pharmacol* **58**: 920–927
Zauber P, Sabbath-Solitare M, Marotta SP, Bishop DT (2003) Molecular changes in the Ki-ras and APC genes in primary colorectal carcinoma and synchronous metastases compared with the findings in accompanying adenomas. *Mol Pathol* **56**: 137–140

Makinoshima et al. BMC Cancer 2012, 12:537
http://www.biomedcentral.com/1471-2407/12/537

BMC Cancer

RESEARCH ARTICLE Open Access

PTPRZ1 regulates calmodulin phosphorylation and tumor progression in small-cell lung carcinoma

Hideki Makinoshima[1,2], Genichiro Ishii[1], Motohiro Kojima[1], Satoshi Fujii[1], Youichi Higuchi[2,3], Takeshi Kuwata[1] and Atsushi Ochiai[1,3*]

Abstract

Background: Small-cell lung carcinoma (SCLC) is a neuroendocrine tumor subtype and comprises approximately 15% of lung cancers. Because SCLC is still a disease with a poor prognosis and limited treatment options, there is an urgent need to develop targeted molecular agents for this disease.

Methods: We screened 20 cell lines from a variety of pathological phenotypes established from different organs by RT-PCR. Paraffin-embedded tissue from 252 primary tumors was examined for PTPRZ1 expression using immunohistochemistry. shRNA mediated *PTPRZ1* down-regulation was used to study impact on tyrosine phosphorylation and *in vivo* tumor progression in SCLC cell lines.

Results: Here we show that PTPRZ1, a member of the protein tyrosine- phosphatase receptor (PTPR) family, is highly expressed in SCLC cell lines and specifically exists in human neuroendocrine tumor (NET) tissues. We also demonstrate that binding of the ligand of PTPRZ1, pleiotrophin (PTN), activates the PTN/PTPRZ1 signaling pathway to induce tyrosine phosphorylation of calmodulin (CaM) in SCLC cells, suggesting that PTPRZ1 is a regulator of tyrosine phosphorylation in SCLC cells. Furthermore, we found that PTPRZ1 actually has an important oncogenic role in tumor progression in the murine xenograft model.

Conclusion: PTPRZ1 was highly expressed in human NET tissues and PTPRZ1 is an oncogenic tyrosine phosphatase in SCLCs. These results imply that a new signaling pathway involving PTPRZ1 could be a feasible target for treatment of NETs.

Keywords: Small cell lung carcinoma (SCLC), Protein tyrosine phosphatase (PTP), Protein tyrosine phosphatase receptor Z1 (PTPRZ1), NETs (Neuroendocrine tumors), Pleiotrophin (PTN), Calmodulin (CaM)

Background

Neuroendocrine tumors (NETs) that includes small cell lung carcinomas (SCLC), large cell neuroendocrine carcinomas (LCNEC), pancreatic neuroendocrine tumors (PanNET), medullary thyroid carcinomas (MTC), pheochromocytomas, paragangliomas, and carcinoids [1-4]. As one of the most malignant NETs, SCLC comprises approximately 15% of lung cancer cases, and basic and clinical research efforts have translated little innovation in the treatment of this disease over the past 30 years [5]. Although SCLC appears to be effectively controlled with first line chemotherapy because of its relative high sensitivity to chemotherapy and radiotherapy, most patients ultimately relapse and salvage chemotherapy is considered [6]. To identify novel drug targets against SCLC, a greater understanding of the pathology of SCLC through molecular analysis is urgently needed.

Dissection of the signaling pathways that may be involved in the regulation of SCLC growth, for example via phosphorylation or dephosphorylation of critical proteins, may shed light on new approaches for tumor

* Correspondence: aochiai@east.ncc.go.jp
[1]Pathology Division, Research Center for Innovative Oncology, National Cancer Center Hospital East, 6-5-1 Kashiwanoha, Kashiwa, Chiba, 277-8577, Japan
[3]Laboratory of Cancer Biology, Department of Integrated Biosciences, Graduate School of Frontier Sciences, The University of Tokyo, Kashiwa, Chiba, Japan
Full list of author information is available at the end of the article

elimination. Protein tyrosine phosphorylation is tightly regulated by protein tyrosine-kinases (PTKs) and protein tyrosine-phosphatases (PTPs) [7,8]. PTPs play an important role in the inhibition and control of growth as tumor suppressors, since aberrant tyrosine phosphorylation is a characteristic feature of cancer cells [7-9]. Indeed, PTPs expressed as cell surface receptors (PTPRs) have been reported to be inactivated by genetic mutations in human cancer [9,10]. On the other hand, there is mounting evidence suggesting that several PTPRs also have oncogenic function [9].

PTPRZ1, as a member of the PTPR family, is a single-pass type I membrane protein with two cytoplasmic tyrosine phosphatase domains (D1 and D2), an alpha-carbonic anhydrase domain (CA), chondroitin sulfate proteoglycans (CS-PGs) and a fibronectin type-III domain (FNIII) [11]. PTPRZ1 interacts with its ligand pleiotrophin (PTN), which is a secreted growth factor involved in angiogenesis and tumor growth [12,13]. Upon binding, PTN inactivates the phosphatase activity of PTPRZ1, which leads to an increased tyrosine phosphorylation status of important signaling molecules such as β-catenin, Fyn and RhoGAP [14-18]. With regard to cancer, PTPRZ1 expression was dramatically induced by genetic amplification caused by chronic oxidative stress and hypoxic stress through HIF-2 alpha [14,19] and several previous studies suggested that PTPRZ1 regulates cancer cell growth and cell migration [18,20-24].

In this paper, we found that PTPRZ1 is highly expressed in SCLC cell lines and specifically exists in human NET tissues. We hypothesized that PTPRZ1 functions to regulate tyrosine phosphorylation in SCLC cells and has an important role for SCLC tumor progression. To test this idea, we investigated the ability of PTPRZ1 to regulate tyrosine phosphorylation and tumor progression using SCLC cell lines.

Methods

Cell cultures

LN229 (glioblastoma, ATCC#CRL-2611), U87MG (glioblastoma/astrocytoma, ATCC#HTB-14), Hela (cervix ADCA, ATCC#CCL-2), Caco2 (colorectal ADCA, ATCC#HTB-37), DLD1 (colorectal ADCA, ATCC#CCL-221), HCT116 (colorectal ADCA, ATCC#CCL-247), SW480 (colorectal ADCA, ATCC#CCL-228), A549 (lung ADCA, ATCC#CCL-185), LNCaP (prostate ADCA, ATCC#CRL-1740), MCF7 (breast ADCA, ATCC#HTB-22), A431 (squamous cell carcinoma, ATCC#CRL-1555), NCI-H69 (SCLC, ATCC#HTB-119), NCI-H82 (SCLC, ATCC#HTB-175), NCI-H345 (SCLC, ATCC#HTB-180), NCI-H446 (SCLC, ATCC#HTB-171), NCI-H510A (SCLC, ATCC#HTB-184), NCI-H1436 (SCLC, ATCC#CRL-5871), and NCI-H1930 (SCLC, ATCC#CRL-5906) were originally purchased from ATCC and stocked in our Research Center. TE1 (esophagus squamous cell carcinoma), TE3 (esophagus squamous cell carcinoma), TE4 (esophagus squamous cell carcinoma), TE5 (esophagus squamous cell carcinoma), and TE10 (esophagus squamous cell carcinoma) were gifts from Dr. Sasaki (National Cancer Center Research Institute). SBC-3 (SCLC, #JCRB0818) was obtained from the JCRB and stocked in our Research Center. All cell lines were cultured in cell culture dishes (BD Biosciences) at 37°C and 5% carbon dioxide using RPMI 1640 (SIGMA), DMEM (SIGMA) supplemented with 10% fetal bovine serum (FBS, Nichirei Bioscience), or HITES Medium [25,26] supplemented with penicillin/streptomycin (Invitrogen). For the PTN assay, 100 ng/ml of recombinant human pleiotrophin/PTN (R&D Systems #252-PL) was used.

Human cancer samples

Samples were obtained with informed consent from each individual, and the study was approved by the Ethics Committee of the National Cancer Center East Hospital. During the period from January 1992 to December 2010, a total of 252 patients who had primary tumors were treated at the National Cancer Center Hospital East, Chiba, Japan. All primary cancers with a pathologic diagnosis based on the classification schema of the WHO classification were reviewed, with 105 cases as adenocarcinoma (ADC), 61 as squamous cell carcinoma (SQCC) and 86 as neuroendocrine tumors (NETs). We used tissue microarray (TMA) to measure PTPRZ1 expression within lung tumors [27]. Each case in which more than 80% of the cancer cells reacted positively for an antibody to PTPRZ1 was recorded as positive.

Antibodies

Antibodies used included anti-PTPRZ1 (SIGMA #015103) [28], anti-Phosphotyrosine, clone 4 G10 (Millipore #05-321), anti-Calmodulin (Santa Cruz sc-5537, Millipore #05-173, abcam ab45689), anti-phospho-Calmodulin (Santa Cruz Biotechnology sc-23760-R, Millipore #09-295) and anti-β-tublin (Cell Signaling #2146).

Immunohistochemistry (IHC)

All immunohistochemical (IHC) analyses were performed on paraffin-embedded tissues obtained from the primary tumor in the surgical specimen. For all IHC analyses the surgically resected specimens were fixed in 10% formalin and embedded in paraffin for routine pathological examination. We prepared and used 5-μm-thick paraffin sections cut from a paraffin block containing histological findings that were representative of the tumor. The procedure for IHC was previously described [27,28]. Antigen retrieval was performed in citrate buffer solution (pH 6.0). Endogenous peroxidase was blocked with 0.3% H_2O_2 in methanol for 15 min and all slides were heated to 95°C by exposure to microwave irradiation for 20 min and then cooled at room temperature (RT). Slides were washed in PBS and after a 1 h incubation at RT with the primary antibodies, the slides were incubated for 30 min with a labeled polymer EnVision TM+, Peroxidase–conjugated anti-Mouse or Rabbit (Dako, Tokyo, Japan). The chromogen used was 2% 3, 3′-diaminobenzidine (DAB) in 50 mM Tris-buffer (pH 7.6) containing 0.3% hydrogen.

RNA isolation and real-time RT–PCR

Cells were washed with PBS and total RNA from the cell lines was isolated with TRIzol Reagent (Invitrogen). Complementary DNA (cDNA) was synthesized using the PrimeScript® RT reagent Kit (TaKaRa, Japan). Real-time RT–PCR was carried out with specific primers and a Smart Cycler (Cepheid, Sunnyvale, CA, USA). Real-time fluorescence monitoring of the PCR products was performed with SYBR Green I fluorescent dye (TaKaRa). The levels of expression of specific genes are reported as ratios to the level of expression of *GAPDH* in the same master reaction. Synthesized primers were purchased from TaKaRa Bio with Primer Set ID given as *PTPRZ1*, 3′ (HA082543). GAPDH was used for normalization as control and the relative quantitation value compared to the calibrator for that target is expressed as $2^{-(Ct-Cc)}$.

Western blot

Western blotting was performed as described [29]. After lentivirus infection with the vector for sh*LUC* or sh*PTPRZ1*, total cell lysate was prepared from cells cultured in complete medium. Primary antibodies were used at 1:1000 dilution and β-tubulin was used as loading control.

Expression of short hairpin RNA (shRNA)

Plasmid construction was carried out with Gateway system (Invitrogen) according to the manufacturer's instructions. Cloning vectors were pDNOR221 (Invitrogen) and pENTR/U6 (Invitrogen). The lentiviruses were produced using 293FT cells (Invitrogen) transfected with pCAG-HIVgp, pCMV-VSV-G-RSV-Rev, and a lentivirus vector based on CSII-CMV-RfA-IRES2-Venus (Dr. Miyoshi, RIKEN BioResource Center) expressing shRNA with the sequence described below. Transfection was achieved using Lipofectamine 2000 reagent (Invitrogen) according to the manufacturer's instructions. Lentivirus-containing medium was filtered through a 0.45 μm filter and used for transduction of target cells. The sequences and plasmid names were; sh*LUC*: GTGCGCTGCTGGTGCCAAC (pGL3, firefly luciferase), sh*PTPRZ1*_1: GCCTATAAATT-GTGAGAGCTT (pHMA017), sh*PTPRZ1*_2: GCTGCTT-TAGATCCATTCATA (pHMA019), and sh*PTPRZ1*_3: GGATGGCAAACTGACTGAT (pHMA022).

Flow cytometry

Cells were incubated with anti-PTPRZ1 antibody (SIGMA) and excess antibody was removed by washing with PBS containing 2% FBS. Polyclonal goat anti-rabbit immunoglobulin conjugated to Phycoerythrin (PE) (Jackson) was added as a secondary antibody. The cells were then washed with PBS and flow cytometric analysis was performed using a FACSCalibur and FACSAria (BD Biosciences).

Animal studies

All of experimental *SCID* mice were handled in accordance with institutional guidelines established by the Animal Care Committee of the National Cancer Center East Hospital. H69 and H1930 SCLC cells expressing shRNA were injected into the subcutaneous tissue of SCID mice (7–8 weeks of age, CLEA, Tokyo, Japan). Tumor volume was calculated as the product of a scaling factor of 0.52 and the tumor length, width, and height were measured every week. For IHC analysis, organs were obtained from mice at 5 or 8 weeks after injection and fixed in 10% formalin.

Statistical methods

Standard Student's *t*-test was used to determine the significance between non-targeting control and sh*PTPRZ1* experiments. Statistical correlation was carried out using χ2test for independence (2 × 2 *contingency table*). $P < 0.05$ was considered statistically significant.

Results

PTPRZ1 is highly expressed in SCLC cell lines

To assess mRNA expression of *PTPRZ1* comprehensively in human cancers, we screened 20 cell lines from a variety of pathological phenotypes established from different organs by RT-PCR. We observed that two SCLC cell lines at the first screening, NCI-H69 (H69) and NCI-H1930 (H1930), expressed *PTPRZ1* mRNA at significantly higher levels than other cell lines (Figure 1A). To confirm the specificity of PTPRZ1 expression in SCLC cells, we measured PTPRZ1 protein levels by Western blotting (Figure 1B). The human *PTPRZ1* gene encodes a core protein consisting of 2315 amino acids (NCBI Reference Sequence: NP_002842) with a predicted molecular weight (M.W.) of 400 kDa, [30]. Indeed, we detected a specific band of PTPRZ1 protein at approximately 400 kDa by WB, only within SCLC cell lines expressing *PTPRZ1* mRNA at high levels (Figure 1B).

PTPRZ1 is specifically expressed in human NET tissues

To determine globally which human tumor tissues expressed PTPRZ1, we analyzed immunohistochemical (IHC) evaluations of a variety of tumors including 105

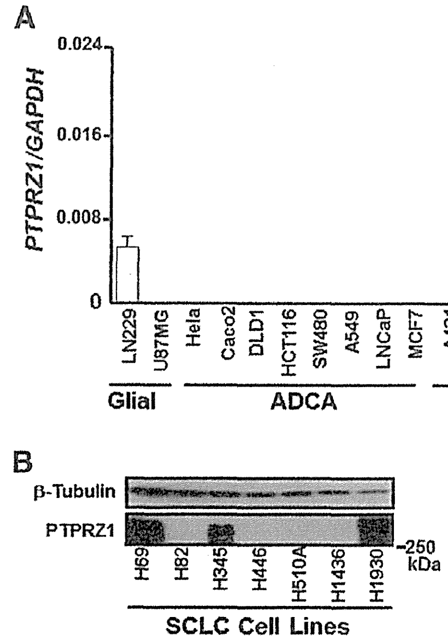

Figure 1 Gene expression of PTPRZ1 among the different cancer cell lines. Glial, adenocarcinoma (ADCA), squamous cell carcinoma (SQCC) and neuroendocrine tumor (NET) cell lines were screened for *PTPRZ1* mRNA levels (normalized to GAPDH), with standard deviation error bars shown (**A**). PTPRZ1 was expressed in SCLC cell lines at protein level (**B**).

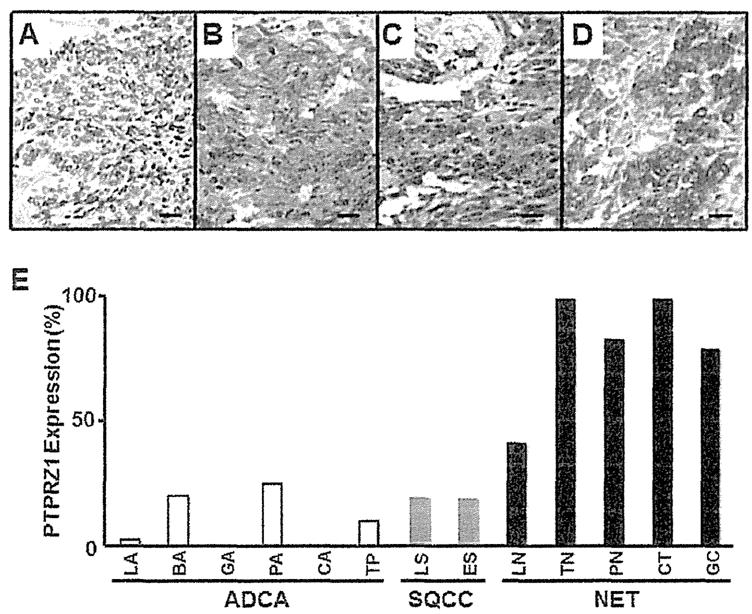

Figure 2 PTPRZ1 was expressed in human NETs. A–D, Representative microscopic images for PTPRZ1-negative SCLC (**A**), PTPRZ1-positive SCLC (**B**), Thyroid Medullary carcinoma (TMC) (**C**) and Pancreatic endocrine tumor (PanNET) (**D**). Scale bars are 20 μm (Magnification X40). **E**, The percentage of PTPRZ1 expression in human tumor tissues was measured in ADCA, SQCC, and NET pathological types including lung ADCA (LA), breast ADCA (BA), gastric ADCA (GA), pancreatic ADCA (PA), colon ADCA (CA), Thyroid ADCA (TA), lung SQCC (LS), esophagous SQCC (ES),lung NET (LN), thyroid NET (TN), pancreatic NET (PN), chromaffin-cell NET (CT), and gastrointestinal carcinoid (GC).